BMC Complementary Medicine and Therapies

RESEARCH

Open Access

Phytochemical analysis and biological effects of *Zingiber cassumunar* extract and three phenylbutenoids: targeting NF-κB, Akt/MAPK, and caspase-3 pathways

Thidaporn Gundom[1], Wanida Sukketsiri[2*] and Pharkphoom Panichayupakaranant[1,3*]

Abstract

Background *Zingiber cassumunar* Roxb., belonging to the Zingiberaceae family, is a medicinal herb commonly found in tropical regions, particularly in Southeast Asia. This research aims to investigate the preventive effects and anti-inflammatory properties of a phenylbutenoid extract (PE) obtained from the rhizomes of *Z. cassumunar*.

Method The PE extract was prepared using green microwave extraction and subsequently analyzed by high-performance liquid chromatography. To evaluate its anti-inflammatory activity, lipopolysaccharide (LPS)-stimulated RAW264.7 cell models were used to measure the release of nitric oxide (NO), tumor necrosis factor-α (TNF-α), and interleukin-1β (IL-1β) using the Griess assay and enzyme-linked immunosorbent assay, respectively. Additionally, the inhibitory effects of PE on apoptosis and reactive oxygen species (ROS) production were evaluated in hydrogen peroxide-induced C2C12 myoblast cells. The expression of inflammation- and apoptosis-related proteins was evaluated using western blotting.

Results The results indicated that the PE was enriched with (*E*)-(3,4-dimethoxyphenyl)butadiene (DMPBD), (*E*)-1-(3,4-dimethoxyphenyl)but-3-en-1-ol (compound D), and (*E*)-1-(3,4-dimethoxyphenyl)but-3-en-1-yl acetate (compound D acetate). The PE contained a total phenylbutenoid content of 1.42% w/w. The PE exhibited potent anti-inflammatory properties, with half maximal inhibitory concentration (IC_{50}) values of 7.2 µg/mL for NO, 23.4 µg/mL for TNF-α, and 19.8 µg/mL for IL-1β. In comparison, DMPBD exhibited lower activity against NO and TNF-α (IC_{50} values of 16.3 and 37.2 µg/mL, respectively) but similar efficacy against IL-1β (IC_{50} of 17.7 µg/mL) in LPS-induced RAW264.7 cells. All test compounds significantly decreased the percentage of apoptotic cells and suppressed intracellular ROS production in hydrogen peroxide-induced C2C12 myoblast cells. Notably, PE exhibited the highest potency in reducing apoptotic cells, with the lowest IC_{50} value of 11.6 µg/mL. PE inhibited the expression of p-p38/p38, pERK/ERK, and pAkt/Akt in the LPS-induced inflammatory response in RAW264.7 cells. Additionally, PE significantly suppressed the cleaved/pro-caspase-3 ratio without affecting Bax and Bcl-2 protein levels.

*Correspondence:
Wanida Sukketsiri
wanida.su@psu.ac.th
Pharkphoom Panichayupakaranant
pharkphoom.p@psu.ac.th

Full list of author information is available at the end of the article

Conclusion These findings suggest that PE and its phenylbutenoids exhibit anti-inflammatory effects through the inhibition of p38, ERK, and Akt signaling pathways, and anti-apoptotic effects via the inhibition of the caspase-3 pathway, highlighting their therapeutic potential for managing inflammatory and degenerative conditions.

Clinical trial number Not applicable.

Keywords Anti-inflammatory, Apoptosis, Phenylbutenoid, *Zingiber cassumunar*

Introduction

Musculoskeletal conditions encompass a variety of injuries and disorders affecting muscles, nerves, tendons, joints, and cartilage, making them the most prevalent global disease in 2019, impacting approximately 1.71 billion individuals [1]. These conditions present major health issues, often resulting from physical exertion, acute trauma, and underlying diseases [2]. Despite musculoskeletal injuries vary widely, the mechanisms of damage and repair share common pathways. Skeletal muscle injury triggers a sequential process involving degeneration, inflammation, regeneration, and fibrosis, highlighting the complexity of musculoskeletal health and recovery [3]. C2C12 cells, a widely used mouse muscle cell line, are instrumental in studying muscle-related diseases, injury, and repair mechanisms [4]. They are particularly valuable for investigating conditions such as sarcopenia and skeletal myopathy, which are often associated with oxidative stress-induced apoptosis [5]. Muscle injury initiates an inflammatory response marked by the secretion of various inflammatory mediators. This includes cytokines such as tumor necrosis factor-α (TNF-α) and interleukin (IL) -1β (IL-1β), as well as free radicals such as nitric oxide (NO) and reactive oxygen species (ROS). For successful skeletal muscle regeneration, it is crucial to promote myoblast proliferation and differentiation, while simultaneously inhibiting apoptosis [6].

Nuclear factor kappa B (NF-κB) is vital for muscle injury and repair. Following injury, NF-κB activation recruits inflammatory cells that are essential for repair. However, excessive NF-κB activation can impair muscle regeneration and contribute to atrophy in conditions such as aging, muscular dystrophy, and cachexia [7]. NF-κB and mitogen-activated protein kinase (MAPK) signaling pathways are intricately associated with inflammation and muscle injury repair processes [8]. MAPKs contribute to cytokine production, including TNF-α and IL-6, and the synthesis of inducible nitric oxide synthase (iNOS) and cyclooxygenase-2 by interfering with NF-κB signaling [9, 10]. Additionally, caspase-3 is crucial for muscle injury and repair, particularly in apoptosis and atrophy. After an injury, caspase-3 activation can lead to myofiber death [11]. Caspase-3 is activated by inflammatory signals, for example, TNF-α and is involved in muscle protein degradation, contributing to muscle loss during catabolic conditions. For instance, in immobilization-induced atrophy, caspase-3 activation is associated with apoptotic myonuclei and mass loss [12].

Zingiber cassumunar Roxb., a member of the Zingiberaceae family, is a medicinal herb primarily found in tropical regions, especially throughout Southeast Asia. In Thai traditional medicine, the rhizomes of this plant are used to treat a variety of ailments, including sprains, rheumatoid arthritis, muscular pain, cutaneous fungal infections, and wounds [13]. The primary active constituents identified in *Z. cassumunar* are phenylbutenoids, including (*E*)-(3,4-dimethoxyphenyl)butadiene (DMPBD), (*E*)-1-(3,4-dimethoxyphenyl)but-3-en-1-ol (compound D), and (*E*)-1-(3,4-dimethoxyphenyl)but-3-en-1-yl acetate (compound D acetate) (Fig. 1) [14] exhibit significant anti-inflammatory and analgesic properties [13, 15–19]. DMPBD and compound D acetate have demonstrated effectiveness in reducing inflammation and pain in vitro and in vivo models [13, 18, 19]. Moreover, the essential oil of *Z. cassumunar* contains compounds like sabinene and terpinen-4-ol, which possess antioxidant activity [20]. These phenylbutenoids serve as bioactive markers for the quantitative analysis of extracts, highlighting their therapeutic potential in treating inflammatory conditions and promoting muscle recovery.

Extraction and standardization are critical processes in preparing herbal extracts. An effective extraction method and suitable solvent are vital for maximizing active constituents, while standardization ensures consistent therapeutic effectiveness [21]. Although hexane is optimal for extracting phenylbutenoids under reflux conditions, its toxicity poses risks to human health and the environment [22]. Recently, green extraction methods have gained considerable attention in the herbal product industry due to their cost-effectiveness and environmental sustainability, with microwave extraction using green solvents being a notable example. Therefore, this study aimed to prepare a phenylbutenoid-enriched extract from *Z. cassumunar* using green microwave extraction with polyethylene glycol (PEG 400) as a solvent, thereby enabling direct formulation. Additionally, the study evaluated the anti-inflammatory effects of the phenylbutenoid extract (PE) on RAW264.7 cells and its cytoprotective effects on C2C12 myoblasts.

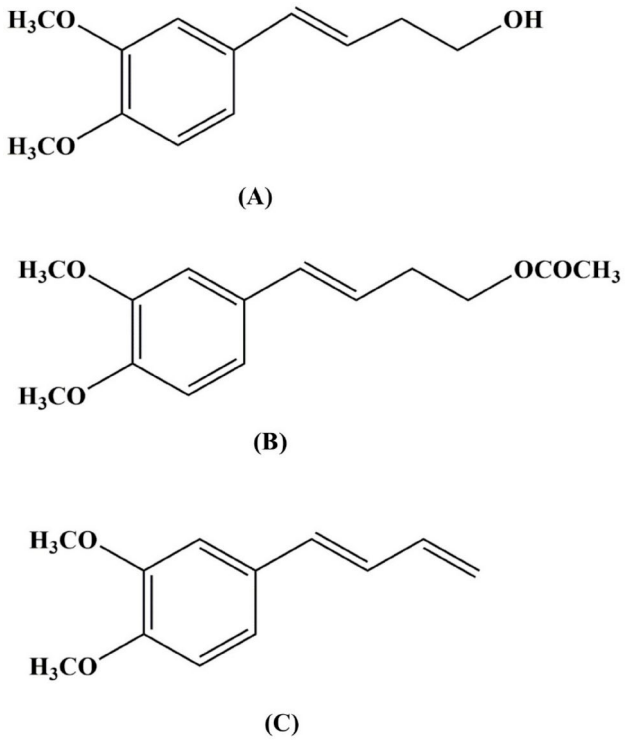

Fig. 1 Chemical structures of (*E*)-1-(3,4-dimethoxyphenyl)but-3-en-1-ol (compound D) **(A)**, (*E*)-1-(3,4-dimethoxyphenyl)but-3-en-1-yl acetate (compound D acetate) **(B)**, and (*E*)-(3,4-dimethoxyphenyl)butadiene (DMPBD) **(C)**

Materials and methods

Drugs and reagents

DMPBD, compound D, and compound D acetate were purified by the method previously described by Kaewchoothong et al. [18]. All chemicals (analytical grade) and high-performance liquid chromatography (HPLC) solvents were obtained from Lab-Scan Asia (Bangkok, Thailand). PEG 400 (cosmetical grade) was purchased from S. Tong Chemicals Co., Ltd. (Nonthaburi, Thailand). Dulbecco's Modified Eagle Medium (DMEM), fetal bovine serum, antibiotics (streptomycin and penicillin), L-glutamine, and trypsin-EDTA (ethylenediaminetetraacetic acid) were purchased from Gibco (Waltham, MA, USA). Enzyme-linked immunosorbent assay (ELISA) kits for IL-1β, and TNF-α were obtained from Merck (Darmstadt, Germany). Lipopolysaccharide (LPS), 3-[4,5-dimethylthiazol-2-yl]-2,5 diphenyl tetrazolium bromide (MTT), 2′-7′- dichlorodihydrofluorescein diacetate ($DCFH_2$-DA), dexamethasone, dimethyl sulfoxide, Hoechst 33342, and N-acetylcysteine (NAC) were obtained from Sigma (St. Louis, MO, USA).

Plant material for phenylbutenoid extract (PE)

The fresh, mature rhizomes of *Z. cassumunar* were purchased from the Saiburi Hatyai Thai herbal store in Songkhla, Thailand, in October 2018. The rhizomes of *Z. cassumunar* were identified by comparing them with an authentic voucher specimen (specimen No. SKP 206 26 03 01) at the Faculty of Pharmaceutical Sciences, Prince of Songkla University, Songkhla, Thailand. The rhizomes were cleaned and cut into small pieces, then dried in a hot air oven at 60 ± 2 °C for 48 h. After drying, the rhizomes were ground into a powder and passed through a sieve (No. 45). The fine powder was stored in a well-closed container at room temperature. A total of 10 kg of dried *Z. cassumunar* powder was extracted using 28 kg of PEG 400 with a microwave extractor from Baan Innov Co., Ltd. in Nakorn Si Thammarat, Thailand. The extraction process was conducted at a power of 4,000 watts, a frequency of 2,450 MHz, and a temperature of 90 ± 5 °C for a duration of 16 min, involving two irradiation cycles, each consisting of 8 min of power-on followed by 2 min of power-off. Following extraction, the mixture was filtered and stored in a light-protected, tightly sealed container, after which it underwent quantitative analysis for phenylbutenoids using HPLC.

Liquid Chromatography-Mass spectrometry

To characterize the phytochemical composition of PE, we employed liquid chromatography and tandem mass spectrometry (LC-MS/MS). The mass spectrometry (MS) parameters were set as follows: electron spray ionization (ESI) in both negative and positive modes, with a capillary voltage of 4,000 V, nozzle voltage of 2,000 V, collision energy (CE) voltage ranging from 10 to 40 V, nebulizer pressure of 35 psi, gas flow rate of 13 L/min at 325 °C, sheath gas flow of 12 L/min at 275 °C, and mass-to-charge ratio (m/z) ranges of 100-1,200 for MS and 50 – 1,200 for MS/MS. The analysis utilized a Zorbax Eclipse Plus C18 reverse phase column, measuring 100 × 2.1 mm with a particle size of 1.8 µm. The PE sample was dissolved in ethanol to achieve a final concentration of 100 mg/mL. Prior to injection, the solution was filtered through a 0.22 µm syringe filter. The injection into the LC-MS/MS system occurred at a flow rate of 0.2 mL/min over a total duration of 32 min. We conducted the analysis using an Ultra-HPLC (UHPLC) system (Agilent Technologies, Inc., California, USA), equipped with an Electrospray Ionization-Quadrupole-Time of Flight Mass Spectrometer. The elution gradients for HPLC included eluent A (0.1% formic acid in water) and eluent B (0.1% formic acid in methanol), following a multistep linear progression: 0–10 min at 5% B, 11–30 min at 100% B, and 31–32 min returning to 5% B, maintained for an additional 5 min. The column temperature was held constant at 25 °C, with an injection volume of 2 µL for both positive and negative ionization modes. MS data were analyzed using Mass Hunter WorkStation Qualitative Analysis Workflows V8 (Agilent Technologies, Inc., California, USA), and identification was facilitated by Mass

Hunter METLIN Metabolite Software, which compared experimental mass spectra against a comprehensive library using weighted similarity scores based on accurate mass values and MS/MS spectra.

Quantitative HPLC method

Chromatographic conditions

Quantitative analysis of phenylbutenoids *via* HPLC was conducted following the protocol established by Kaewchoothong et al. [18], with slight modifications. The analysis utilized a Shimadzu LC-20 A Series system, which included an SPD-M20A photodiode array detector and a SIL-20AHT autosampler (Shimadzu, Tokyo, Japan). An ACE® C18-PFP column (5 µm, 4.6 × 150 mm i.d.) was employed, with a mobile phase composed of methanol (A) and 2% acetic acid in water (B), utilizing a gradient elution method: from 0 to 20 min, A was at 52% v/v; from 22 to 38 min, A decreased to 50% v/v; and from 40 to 60 min, A returned to 52% v/v, all at a flow rate of 1.0 mL/min. The wavelength used for quantification was established at 254 nm. The HPLC method was previously validated for its linearity, specificity, accuracy, repeatability, reproducibility, limits of detection (LOD), and limits of quantification (LOQ) in accordance with the International Council for Harmonization (ICH) guidelines [18]. The protocol for method validation is presented in the supplementary material file.

Standard Preparation

A working solution of three standard compounds, including compound D, compound D acetate, and DMPBD, was freshly prepared in methanol and then diluted to create five different concentrations of the standard solutions (12.5–200 µg/mL). The calibration curve of each standard compound was constructed by plotting peak areas versus concentrations. The calibration curves of compound D, compound D acetate, and DMPBD were $Y = 102558X + 78532$ ($r^2 = 1.0000$), $Y = 75146X + 67079$ ($r^2 = 0.9999$), and $Y = 21921X + 1085.7$ ($r^2 = 0.9999$), respectively.

Cell lines and culture conditions

RAW264.7 and C2C12 myoblast cell lines were purchased from the American Type Culture Collection in Manassas, VA, USA. Both cell lines were grown in DMEM medium enriched with 10% fetal bovine serum, 1% penicillin-streptomycin, and 1% L-glutamine. The cultures were incubated at 37 °C in a humidified environment with 5% CO_2.

Cytotoxicity assay

RAW264.7 and C2C12 myoblast cells were plated at a density of 2×10^4 cells per well in a 96-well plate. Cells were treated with compound D, compound D acetate, DMPBD, and PE at various concentrations ranging from 0.1 to 100 µg/mL for a duration of 24 h. After the treatment period, a volume of 100 µL of 0.5 mg/mL MTT solution was added to each well and incubated for 4 h at 37 °C. The colorimetric MTT assay was then employed to assess cell viability post-treatment. The absorbance of the formazan solution was recorded at 570 nm with a microplate reader (Bio-Tek Instruments, Inc., VT, USA), and the percentage of cell viability was calculated by comparing it to the absorbance of untreated control cells [10].

$$\%\ \text{Viability} = \frac{\text{Mean OD of treated cell}}{\text{Mean OD of untreated cell (control)}} \times 100 \quad (1)$$

Anti-inflammatory assays

Determination of NO production

RAW264.7 cells were seeded at a density of 1×10^5 cells per well and treated with DMPBD, compound D, and compound D acetate at concentrations of 10–100 µg/mL. Additionally, PE was administered at concentrations of 5, 10, 25, and 50 µg/mL. After treatment, the cells were exposed to 1 µg/mL of LPS for 24 h. The NO assay was conducted according to our previously described method [10]. Following this exposure, a volume of 100 µL of the culture medium was collected and combined with an equal amount of Griess reagent. The optical density of the resulting solution was then detected using a microplate reader (Bio-Tek Instruments, Inc., VT, USA) at 540 nm. A standard curve was created using sodium nitrite solutions ranging from 1 to 50 µM. Dexamethasone at a concentration of 1 µg/mL was used as a positive control. The percentage of inhibition was calculated using a specific formula, and IC_{50} values were determined accordingly [18].

$$\%\ \text{Inhibition} = \frac{A - B}{A - C} \times 100 \quad (2)$$

Concentration of NO (µM); A: LPS present (+), sample absent (-); B: LPS present (+), sample present (+); C: LPS absent (-), sample absent (-).

Determination of TNF-α and IL-1β production

RAW264.7 cells were plated at a density of 1×10^5 cells per well and exposed to LPS at a concentration of 1 µg/mL, either alone or in combination with DMPBD, compound D, and compound D acetate at concentrations of 10–100 µg/mL. PE was administered at concentrations of 5–50 µg/mL, while dexamethasone was treated at a concentration of 1 µg/mL. The treatments were conducted for a duration of 24 h. The concentrations of TNF-α and IL-1β in the culture supernatant were then evaluated using an ELISA kit. The percentage of inhibition was

determined using a specified formula, and IC_{50} values were calculated as [18].

$$\%\ \text{Inhibition} = \frac{\text{A - B}}{\text{A - C}} \times 100 \quad (3)$$

Concentration of TNF or IL-1β (pg/mL); A: LPS present (+), sample absent (-); B: LPS present (+), sample present (+); C: LPS absent (-), sample absent (-).

Immunofluorescence

RAW264.7 cells were exposed to LPS either with or without the presence of compound D, compound D acetate, DMPBD, PE, and dexamethasone for 24 h. After stimulation, the cells were fixed using 4% paraformaldehyde for 20 min. To eliminate any excess fixative, the cells were rinsed twice with phosphate-buffered saline. The immunofluorescence protocol was performed according to Sukketsiri et al. [10] with slight modifications. In brief, cells were permeabilized with 0.1% Triton X-100 for 20 min. To avoid nonspecific binding, the cells were blocked with 1% bovine serum albumin for one hour. Subsequently, the cells were incubated with a primary antibody targeting NF-κB (Santa Cruz Biotechnology, diluted 1:200) overnight at 4 °C. Cells were rinsed to remove any unbound antibodies and then incubated for 1 h at room temperature with Alexa Fluor 488® secondary antibodies. To counterstain the nuclei, Hoechst 33342 was applied at a concentration of 10 μg/mL. Finally, the cells were examined using a fluorescence microscope (Olympus IX73, Japan).

Preventive effect on cellular injured C2C12 myoblast cells

Determination of apoptosis

Apoptosis was assessed using the fluorescent DNA stain Hoechst 33342, as described in our previous study [23]. C2C12 myoblast cells were plated in a 6-well plate with a density of 1×10^5 cells per well and then exposed to compound D, compound D acetate, DMPBD, and PE at concentrations of 10–100 μg/mL for 24 h. Following treatment, the cells were subjected to hydrogen peroxide (H_2O_2) at a concentration of 0.5 mM for 2 h. The cells were subsequently fixed at room temperature with 4% paraformaldehyde for 10 min and then stained with 10 μg/mL Hoechst 33342 for 30 min. A concentration of 50 mM of N-acetylcysteine (NAC) was utilized as a positive control. Apoptotic cells, which were identified by chromatin condensation and fragmented nuclei, were visualized using a fluorescence microscope (Olympus IX71, Japan). Five random visual fields were selected from each sample, and data were collected from four independent experiments. The quantity of apoptotic cells was determined and the inhibition percentage was calculated using a designated formula with IC_{50} values determined graphically.

$$\%\text{Inhibition} = \frac{A - B}{A} \times 100 \quad (4)$$

Apoptosis cell (%); A: H_2O_2 (+), sample (-); B: H_2O_2 (+), sample (+).

Determination of ROS production

C2C12 myoblast cells were seeded at a density of 1×10^5 cells per well were pretreated with compound D, compound D acetate, DMPBD, and PE for 24 h before being exposed to H_2O_2 at a concentration of 0.5 mM for 2 h. A concentration of 50 mM of NAC was utilized as a positive control. To evaluate the production of intracellular ROS, the cells were incubated with $DCFH_2$-DA (20 μM) for 45 min in the dark. The fluorescence intensity was then measured using a fluorescence microplate reader (Bio-Tex Instruments, Inc., VT, USA), with an excitation wavelength of 485 nm and an emission wavelength of 530 nm. The percentage of ROS production was calculated as [10].

$$\%\ \text{ROS production} = \frac{\text{B - A}}{\text{A}} \times 100 \quad (5)$$

Absorbance of ROS level; A: H_2O_2 (+), sample (-); B: H_2O_2 (+), sample (+).

Western blot analysis

RAW264.7 cells were exposed to LPS either with or without the addition of compound D, compound D acetate, DMPBD, and PE at a concentration of 50 μg/mL for 24 h. C2C12 cells were pretreated with the same compounds at 50 μg/mL for 24 h before being exposed to H_2O_2 at a concentration of 0.5 mM for 2 h. The protein extracts from RAW264.7 and C2C12 cells were analyzed using 10% sodium dodecyl sulfate-polyacrylamide gel electrophoresis. After electrophoresis, the proteins were transferred to a polyvinylidene fluoride membrane and blocked to reduce non-specific binding. The membranes were subsequently incubated at 4 °C overnight with primary antibodies targeting protein kinase B (Akt), pAkt, extracellular signal-regulated kinase (ERK), pERK, p38, p-p38, B-cell lymphoma protein 2 (Bcl-2), Bcl-2-associated X (Bax), procaspase-3, cleaved-caspase-3, NF-κB, iNOS, and β-actin. All antibodies utilized in this study were sourced from Santa Cruz Biotechnology, CA, USA. The membrane was rinsed with TBST (Tris-buffered saline containing Tween-20) and subsequently incubated with horseradish peroxidase-conjugated secondary antibody at room temperature for 2 h. Protein bands were visualized using an enhanced chemiluminescence substrate

for western blotting and analyzed using ImageJ software (NIH, Maryland).

Statistical analysis

The data are expressed as mean ± SEM from four independent experiments. Statistical analysis was conducted using one-way analysis of variance (ANOVA) followed by LSD post-hoc test. A *p*-value of less than 0.05 was considered statistically significant.

Results

Phytochemical content in the phenylbutenoid extract (PE)

A green microwave extraction of phenylbutenoids from dried powders of *Z. cassumunar* was achieved using PEG 400 as an alternative green solvent. A dark yellowish oily extract of phenylbutenoids in PEG 400 was obtained from 10 kg of dried powders, resulting in an extraction yield of approximately 49.73% w/w for the phenylbutenoid extract. In this study, a variety of chemical constituents in the PE were identified based on their MS/MS fragmentation patterns and the chemical structures of compounds previously reported from this species. The analysis revealed the presence of various compounds, including phenylbutenoids, phenylbutenoid dimers, and curcuminoids. Additionally, polysaccharides and fatty acids were also detected in the PE (Table 1; Fig. 2). The results highlighted numerous bioactive compounds within the PE, including DMPBD, (*E*)-4-(3,4-dimethoxyphenyl)but-3-ene-1-yl acetate, curcumin, (*E*)-1-(2,4,5-trimethoxyphenyl)but-1-ene, cis-3-(2,4,5-trimethoxyphenyl)-4-[(*E*)-2,4,5-trimethoxystyryl] cyclohex-1-ene, cis- or trans-3-(2,4,5-trimethoxyphenyl)-4-[(*E*)-3,4-dimethoxystyryl]cyclohex-1-ene, cis-3-(3,4-dimethoxyphenyl)-4-[(*E*)-2,4,5-trimethoxystyryl] cyclohex-1-ene, and cis-1,2-bis-[(*E*)-3,4-dimethoxystyryl] cyclobutene (Table 1; Fig. 2). For HPLC analysis, PE contained three phenylbutenoids: compound D, compound D acetate, and DMPBD (Fig. 3). The validation data for the quantitative HPLC method for compound D, compound D acetate, and DMPBD are presented in Table S1. Based on HPLC analysis, the extract was composed of 0.93% w/w DMPBD, 0.28% w/w compound D, and 0.21% w/w compound D acetate, resulting in a total phenylbutenoid content of 1.42 ± 0.03% w/w (Table 2).

Effect on the viability of RAW264.7 and C2C12 myoblast cells

Based on the MTT assay, compound D, compound D acetate, and DMPBD exhibited no significant cytotoxicity (cell viability > 80%) on RAW264.7 cells at concentrations up to 100 µg/mL. Meanwhile, PE exhibited no significant cytotoxic effect at concentrations up to 50 µg/mL (Additional file 1: Fig. S1(A)). Similarly, all samples revealed no significant toxicity on C2C12 myoblast cells at concentrations up to 100 µg/mL (Additional file 1: Fig. S1(B)).

Anti-inflammatory effects on RAW264.7 cells

Effect of three phenylbutenoids and PE on NO production and iNOS expression in LPS-induced inflammation in macrophages

The effect of three phenylbutenoids and PE on NO production was assessed in the supernatant of RAW264.7 cells after treatment with 1 µg/mL of LPS and various concentrations of three phenylbutenoids and PE. Figure 4(A-D) illustrates that LPS treatment significantly increased intracellular NO levels in RAW264.7 cells. However, compound D, compound D acetate, and DMPBD at concentrations of 10, 25, 50, and 100 µg/mL, as well as PE at 5, 10, 25, and 50 µg/mL and dexamethasone, significantly reduced NO levels compared to LPS treatment alone ($p < 0.05$). Notably, PE showed a more potent inhibitory effect than the three phenylbutenoids, with an IC_{50} value of 7.2 µg/mL (Table 3). Additionally, the LPS-treated group exhibited the highest expression of iNOS protein in comparison to the control group. Treatment with three phenylbutenoids and PE resulted in a significant reduction in iNOS protein expression compared to the LPS group ($p < 0.05$) (Fig. 4(E-F)). These findings indicate that three phenylbutenoids and PE reduce NO secretion by downregulating the expression of the iNOS protein, which in turn diminishes NO-related inflammation.

Effects of three phenylbutenoids and PE on the secretion of TNF-α and IL-1β in LPS-induced inflammation in macrophages

The release of TNF-α and IL-1β was evaluated using ELISA, and the results are shown in Fig. 5(A-D). LPS-stimulated RAW264.7 cells demonstrated a marked increase in the production of TNF-α and IL-1β when compared to the control group ($p < 0.05$). Regarding TNF-α inhibition, compound D, compound D acetate, DMPBD, and PE were evaluated for their effects on LPS-induced the release of TNF-α, as shown in Fig. 5(A-D) and Table 3. All tested samples demonstrated a reduction in TNF-α levels, with PE exhibiting the most substantial inhibitory effect with an IC_{50} value of 23.4 µg/mL (Table 3). The inhibitory effects of compound D, compound D acetate, DMPBD, and PE on LPS-induced IL-1β release are summarized in Fig. 5(A-D) and Table 3. Among these, PE and DMPBD exhibited the most potent inhibitory effects, with IC_{50} values of 19.8 and 17.7 µg/mL, respectively. These results indicate that all tested phenylbutenoids and PE can inhibit inflammation in macrophages by inhibiting the release of the TNF-α and IL-1β proinflammatory cytokines.

Table 1 MS and MS/MS data of phytochemical compounds detected in PE obtained by UHPLC-ESI-Q-TOF-MS/MS in positive and negative modes

No.	RT (min)	Identification	Molecular formula	Experimental mass (m/z)	Error (ppm)	Adducts
Negative mode						
1	1.406	D-Lactose	$C_{12}H_{22}O_{11}$	377.0855	0.39	(M + Cl)-
2	1.431	Sucrose	$C_{12}H_{22}O_{11}$	341.1089	-0.05	(M-H)-
3	1.682	Sarmentosin epoxide	$C_{11}H_{17}NO_8$	290.0881	-0.14	(M-H)-
4	1.707	(R)-(+)-2-Pyrrolidone-5-carboxylic acid	$C_5H_7NO_3$	128.0353	0.24	(M-H)-
5	1.731	Pseudouridine	$C_9H_{12}N_2O_6$	243.0622	-0.09	(M-H)-
6	6.241	3,4-Dihydroxybenzaldehyde	$C_7H_6O_3$	137.0243	0.44	(M-H)-
7	6.517	Gln Pro Pro	$C_{15}H_{24}N_4O_5$	339.1664	3.06	(M-H)-
8	6.617	dolichyl diphosphate	$C_{25}H_{46}O_7P_2$	519.266	-2.4	(M-H)-
9	8.346	PIP(18:1(9Z)/16:0)	$C_{43}H_{82}O_{16}P_2$	915.5015	-1.21	(M-H)-
10	8.86	PIP(20:1(11Z)/16:0)	$C_{45}H_{86}O_{16}P_2$	943.5328	-1.01	(M-H)-
11	9.285	ethyl 6,7-dimethoxy-4-oxo-2,3-dihydro-1 H-naphthalene-2-carboxylate	$C_{15}H_{18}O_5$	277.1084	-1.09	(M-H)-
12	9.574	(7'x,8'x)-4,7'-Epoxy-3,8'-bilign-7-ene-3,5'-dimethoxy-4',9,9'-triol	$C_{20}H_{22}O_6$	357.1344	-1.16	(M-H)-
13	9.624	Glicoricone	$C_{21}H_{20}O_6$	367.1188	-1.16	(M-H)-
14	9.649	cis-4-Hydroxyequol	$C_{15}H_{14}O_4$	257.0819	-0.49	(M-H)-
15	9.799	2-Methoxyestrone 3-glucuronide	$C_{25}H_{32}O_9$	475.197	0.89	(M-H)-
16	9.924	5-[[4-(4-fluorophenyl)-3-piperidinyl]methoxy]-2-methoxy-, (3 S-trans)-Phenol glucuronide	$C_{25}H_{30}FNO_9$	506.1819	1.53	(M-H)-
17	9.937	Curcumin	$C_{21}H_{20}O_6$	367.1191	-1.62	(M-H)-
18	10	Lepidissipyrone	$C_{24}H_{22}O_7$	421.1293	-1.32	(M-H)-
19	10.087	Calebin A	$C_{21}H_{20}O_7$	383.1138	-1.33	(M-H)-
20	10.1	6,8-Dihydroxy-1,7-diprenylxanthone-2-carboxylic acid	$C_{24}H_{24}O_6$	407.1501	0.05	(M-H)-
21	10.325	(+)-Tephropurpurin	$C_{24}H_{24}O_7$	423.1451	-3.27	(M-H)-
22	10.401	Mangostenol	$C_{24}H_{26}O_7$	425.1609	-1.05	(M-H)-
23	10.438	Kanzonol Q	$C_{15}H_{16}O_4$	259.0976	-0.32	(M-H)-
24	10.764	Epoxy (4,5α)-4,5-Dihydrosantonin	$C_{15}H_{18}O_4$	261.1133	-0.45	(M-H)-
25	10.902	Valdiate	$C_{17}H_{26}O_5$	309.1707	1.06	(M-H)-
26	10.939	9 S,10 S,11R-trihydroxy-12Z-octadecenoic acid	$C_{18}H_{34}O_5$	329.2331	0.52	(M-H)-
27	11.027	1,2,3,4-Tetrahydro-1-[1-hydroxy-3-(4-hydroxyphenyl)-2-propenyl]-7-methoxy-2,6-naphthalenediol	$C_{20}H_{22}O_5$	341.1393	0.8	(M-H)-
28	11.102	Curcumin	$C_{21}H_{20}O_6$	367.1187	-0.22	(M-H)-
29	11.127	Piperic acid	$C_{12}H_{10}O_4$	217.0509	-0.69	(M-H)-
30	11.252	Valdiate	$C_{17}H_{26}O_5$	309.1709	-0.11	(M-H)-
31	11.265	Myrsinone	$C_{17}H_{26}O_4$	293.1757	0.44	(M-H)-
32	11.428	12-Dehydroporson	$C_{22}H_{24}O_6$	383.1504	-0.72	(M-H)-
33	12.004	Olmesartan Medoxomil	$C_{29}H_{30}N_6O_6$	557.218	-4.98	(M-H)-
34	12.054	8-HpODE	$C_{18}H_{32}O_4$	311.2227	0.47	(M-H)-
35	12.255	13(S)-HOTrE	$C_{18}H_{30}O_3$	293.2122	-0.39	(M-H)-
36	12.505	9(R)-HODE	$C_{18}H_{32}O_3$	295.2276	0.72	(M-H)-
37	12.53	3,4-Dimethyl-5-pentyl-2-furanheptanoic acid	$C_{18}H_{30}O_3$	293.212	0.72	(M-H)-
38	12.806	trans-Δ2-11-methyl-Dodecenoic Acid	$C_{13}H_{24}O_2$	211.17	1.67	(M-H)-
39	12.906	Amoricin	$C_{31}H_{36}O_6$	503.2439	0.28	(M-H)-
40	13.332	16-hydroxy hexadecanoic acid	$C_{16}H_{32}O_3$	271.2275	1.32	(M-H)-
41	13.357	Pinolenic Acid	$C_{18}H_{30}O_2$	277.2173	-0.33	(M-H)-
42	13.457	(+)-Isomyristic acid	$C_{14}H_{28}O_2$	227.2014	0.92	(M-H)-
43	13.507	Δ2-cis-Hexadecenoic Acid	$C_{16}H_{30}O_2$	253.2169	1.7	(M-H)-
44	13.532	1α-hydroxy-23-[3-(1-hydroxy-1-methylethyl)phenyl]-22,22,23,23-tetradehydro-24,25,26,27-tetranorvitamin D3 / 1α-hydroxy-23-[3-(1-hydroxy-1-methylethyl) phenyl]-22,22,23,23-tetradehydro-24,25,26,27-tetranorcholecalciferol	$C_{32}H_{42}O_3$	473.3053	1.8	(M-H)-
45	13.708	10E,12Z-Octadecadienoic acid	$C_{18}H_{32}O_2$	279.2327	0.64	(M-H)-

Table 1 (continued)

No.	RT (min)	Identification	Molecular formula	Experimental mass (m/z)	Error (ppm)	Adducts
46	14.033	Isopalmitic acid	$C_{16}H_{32}O_2$	255.2327	0.94	(M-H)-
47	14.159	Vaccenic acid	$C_{18}H_{34}O_2$	281.2483	0.86	(M-H)-
48	14.334	5(Z),14(Z)-Eicosadienoic Acid	$C_{20}H_{36}O_2$	307.2638	1.59	(M-H)-
Positive mode						
1	3.346	Nordihydrocapsaicin	$C_{17}H_{27}NO_3$	294.2053	3.78	(M + H)+
2	4.824	Acetylagmatine	$C_7H_{16}N_4O$	195.1223	-4.21	(M + Na)+
3	5.638	N-omega-propyl-L-Arginine	$C_9H_{20}N_4O_2$	239.1487	-4.49	(M + Na)+
4	5.726	Isopropyl beta-D-glucoside	$C_9H_{18}O_6$	245.0993	1.16	(M + Na)+
5	6.052	Met Gly Asn	$C_{11}H_{20}N_4O_5S$	161.065	-0.61	(M + 2 H) + 2
6	6.403	Ser Ser Arg	$C_{12}H_{24}N_6O_6$	349.1836	-2.12	(M + H)+
7	6.428	Istamycin AP	$C_{13}H_{28}N_4O_4$	327.2017	-4.84	(M + Na)+
8	6.603	Ser Ser Arg	$C_{12}H_{24}N_6O_6$	349.183	-0.43	(M + H)+
9	6.628	Istamycin AP	$C_{13}H_{28}N_4O_4$	327.2014	-3.67	(M + Na)+
10	6.804	(6RS)-22-oxo-23,24,25,26,27-pentanorvitamin D3 6,19-sulfur dioxide adduct / (6RS)-22-oxo-23,24,25,26,27-pentanorcholecalciferol 6,19-sulfurdioxide adduct	$C_{22}H_{32}O_4S$	393.21	-1.67	(M + Na)+
11	6.829	1-epi-Fortimicin B	$C_{15}H_{32}N_4O_5$	371.2279	-4.14	(M + Na)+
12	6.853	Gln Leu Lys	$C_{17}H_{33}N_5O_5$	388.2548	1.5	(M + H)+
13	7.104	Istamycin C1	$C_{19}H_{37}N_5O_6$	432.2803	2.88	(M + H)+
14	7.317	Arg Gln Arg	$C_{17}H_{34}N_{10}O_5$	481.2622	-3.73	(M + Na)+
15	7.317	Arg Gln Arg	$C_{17}H_{34}N_{10}O_5$	459.2804	-4.04	(M + H)+
16	7.354	(14alpha,17beta,20 S,22R)-14,20-Epoxy-17-hydroxy-1-oxowitha-3,5,24-trienolide	$C_{28}H_{36}O_5$	249.1175	-0.28	(M + 2Na) + 2
17	7.605	PG(17:1(9Z)/0:0)	$C_{23}H_{45}O_9P$	271.1303	-4.04	(M + H)+
18	7.781	Ceanothine E	$C_{34}H_{40}N_4O_4$	569.3143	-3.46	(M + 2Na) + 2
19	7.805	Ciclesonide	$C_{32}H_{44}O_7$	293.1439	-0.71	(M + 2Na) + 2
20	7.956	Huratoxin	$C_{34}H_{48}O_8$	315.157	-0.38	(M + 2Na) + 2
21	8.156	PI(20:0/0:0)	$C_{29}H_{57}O_{12}P$	337.1699	-3.82	(M + 2Na) + 2
22	8.507	PA(20:5(5Z,8Z,11Z,14Z,17Z)/22:6(4Z,7Z,10Z,13Z,16Z,19Z))	$C_{45}H_{67}O_8P$	789.4444	2.96	(M + 2Na) + 2
23	8.532	PA(18:2(9Z,12Z)/22:6(4Z,7Z,10Z,13Z,16Z,19Z))	$C_{43}H_{69}O_8P$	767.4624	-0.41	(M + Na)+
24	8.557	PA(20:5(5Z,8Z,11Z,14Z,17Z)/22:6(4Z,7Z,10Z,13Z,16Z,19Z))	$C_{45}H_{67}O_8P$	384.235	2.13	(M + Na)+
25	8.708	Pectenotoxin 2 secoacid	$C_{47}H_{72}O_{15}$	877.4968	-2.94	(M + H)+
26	8.733	PG(22:4(7Z,10Z,13Z,16Z)/17:1(9Z))	$C_{45}H_{79}O_{10}P$	428.2612	-3.8	(M + 2Na) + 2
27	8.758	Pectenotoxin 2 secoacid	$C_{47}H_{72}O_{15}$	439.2522	-2.89	(M + 2 H) + 2
28	8.833	Hebevinoside XIII	$C_{49}H_{76}O_{16}$	461.2652	-2.56	(M + 2 H) + 2
29	8.858	Hebevinoside XIII	$C_{49}H_{76}O_{16}$	921.5232	-2.71	(M + H)+
30	8.908	PI(P-20:0/20:4(5Z,8Z,11Z,14Z))	$C_{49}H_{87}O_{12}P$	472.2872	-2.88	(M + 2Na) + 2
31	9.009	PI(22:4(7Z,10Z,13Z,16Z)/20:0)	$C_{51}H_{91}O_{13}P$	494.3009	-3.46	(M + 2Na) + 2
32	9.058	PI(22:6(4Z,7Z,10Z,13Z,16Z,19Z)/22:1(11Z))	$C_{53}H_{89}O_{13}P$	505.2921	-1.09	(M + 2Na) + 2
	9.259	Cinnamyl propionate	$C_{12}H_{14}O_2$	191.1064	1.17	(M + H)+
34	10.261	1-(3,4-Dihydroxyphenyl)-7-(4-hydroxy-3-methoxyphenyl)-1,6-heptadiene-3,5-dione	$C_{20}H_{18}O_6$	377.0991	1.33	(M + Na)+
35	10.412	Moracin L	$C_{19}H_{16}O_5$	347.0885	1.6	(M + Na)+
36	10.612	Cinnamyl propionate	$C_{12}H_{14}O_2$	191.1064	1.49	(M + H)+
37	10.637	Helinorbisabone	$C_{14}H_{18}O_4$	273.1091	2.43	(M + Na)+
38	11.013	Albafuran B	$C_{24}H_{26}O_4$	379.1897	2.03	(M + H)+
39	11.038	(S)-(E)-8-(3,6-Dimethyl-2-heptenyl)-4′,5,7-trihydroxyflavanone	$C_{24}H_{28}O_5$	419.1824	-0.15	(M + Na)+
40	11.138	Kamolonol	$C_{24}H_{30}O_5$	421.1978	2.02	(M + Na)+
41	11.163	Curcumin	$C_{21}H_{20}O_6$	369.1327	1.49	(M + H)+
42	11.314	Cinnamyl propionate	$C_{12}H_{14}O_2$	191.1063	1.93	(M + H)+
43	11.514	Kamolonol	$C_{24}H_{30}O_5$	421.1976	2.55	(M + Na)+
44	11.639	Isoamyl p-anisate	$C_{13}H_{18}O_3$	223.1324	2.18	(M + H)+
45	11.664	Olmesartan Medoxomil	$C_{29}H_{30}N_6O_6$	559.2317	-3.11	(M + H)+
46	11.715	2-(2-Furanyl)-3-methyl-2-butenal	$C_9H_{10}O_2$	151.075	2.91	(M + H)+

Table 1 (continued)

No.	RT (min)	Identification	Molecular formula	Experimental mass (m/z)	Error (ppm)	Adducts
47	11.965	5,7-Dihydroxy-4′-methoxy-8-C-prenyl-3′-(3-hydroxy-3-methylbutyl)flavanone	$C_{26}H_{32}O_6$	463.2081	1.99	(M + Na)+
48	12.516	Heliocide H2	$C_{25}H_{30}O_5$	433.1979	1.57	(M + Na)+
49	12.516	2-Geranyl-3,4,2′,4′-tetrahydroxydihydrochalcone	$C_{25}H_{30}O_5$	411.2161	1.5	(M + H)+
50	12.729	Tokinolide A	$C_{24}H_{28}O_4$	381.2054	1.61	(M + H)+
51	12.754	14-Methoxy-4,4-Bisnor-4,8,11,13-Podocarpatetraen-3-One	$C_{16}H_{18}O_2$	243.1374	2.38	(M + H)+
52	13.268	(±)7-HDoHE	$C_{22}H_{32}O_3$	367.2236	2.67	(M + Na)+
53	13.368	Lucyin A	$C_{30}H_{46}O_5$	509.3221	3.5	(M + Na)+
54	13.418	21-Hydroxyisoglabrolide	$C_{30}H_{44}O_5$	507.3067	2.68	(M + Na)+
55	13.919	PA(17:0/0:0)	$C_{20}H_{41}O_7P$	425.2649	3.14	(M + H)+
56	14.671	BIX01294	$C_{28}H_{38}N_6O_2$	491.312	1.81	(M + H)+
57	14.871	13E-Docosenamide	$C_{22}H_{43}NO$	338.3407	3.06	(M + H)+
58	14.971	(24RS)-28,28,28-trifluoro-25-hydroxyvitamin D2 / (24RS)-28,28,28-trifluoro-25-hydroxyergocalciferol	$C_{28}H_{41}F_3O_2$	467.3116	2.71	(M + H)+
59	15.222	PA(22:1(11Z)/0:0)	$C_{25}H_{49}O_7P$	493.3276	2.53	(M + H)+
60	15.247	6-Deoxodolichosterone	$C_{28}H_{48}O_4$	471.3458	-2.71	(M + Na)+
61	15.836	Secasterone	$C_{28}H_{46}O_4$	469.3279	2.33	(M + Na)+
62	15.861	Cinnamyl propionate	$C_{12}H_{14}O_2$	191.106	2.7	(M + H)+
63	15.873	Secasterone	$C_{28}H_{46}O_4$	447.3456	3.04	(M + H)+
64	16.024	Maslinic Acid	$C_{30}H_{48}O_4$	495.3433	2.64	(M + Na)+
65	16.074	ergosta-3beta,5alpha,6beta,25-tetrol	$C_{28}H_{50}O_4$	473.3608	-1.35	(M + Na)+
66	16.274	3,6,9-Heptacosatriene	$C_{27}H_{50}$	397.3814	-2.47	(M + Na)+
67	16.287	Schottenol 3-glucoside	$C_{35}H_{60}O_6$	599.4265	3.17	(M + Na)+
68	16.976	cholesteryl hemisuccinate	$C_{31}H_{50}O_4$	509.3583	3.67	(M + Na)+
69	17.277	20,24-Epoxy-25,26-dihydroxydammaran-3-one	$C_{30}H_{50}O_4$	497.359	2.47	(M + Na)+
70	18.654	GlcCer(d16:2(4E,6E)/22:0(2OH))	$C_{44}H_{83}NO_9$	792.5933	3.81	(M + Na)+
71	20.057	18Z,21Z-Heptacosadien-10-one	$C_{27}H_{50}O$	413.3763	-2.01	(M + Na)+

Three phenylbutenoids and PE inhibited NF-κB p65 translocation in LPS-induced macrophages

To examine the anti-inflammatory mechanisms of the three phenylbutenoids and PE, we examined their effect on the activation of NF-κB in RAW264.7 cells stimulated with LPS. The nuclear translocation of NF-κB p65 was evaluated using immunofluorescence assays, as illustrated in Fig. 6. The three phenylbutenoids, PE, and dexamethasone reduced the intensity of NF-κB p65 nuclear staining, indicating that these compounds inhibited the movement of NF-κB p65 from the cytoplasm to the nucleus in LPS-inflamed RAW264.7 cells. These results imply that the three phenylbutenoids and PE might block the activation of the NF-κB signaling pathway, resulting in a reduction of inflammation.

Three phenylbutenoids and PE inhibits inflammation by suppressing the ERK, p38 MAPK, and Akt pathways

As illustrated in Fig. 7, the expression levels of pERK/ERK, p-p38/p38, and pAkt/Akt were significantly increased after LPS treatment. However, treatment with the three phenylbutenoids and PE significantly reduced the ratios of pERK/ERK, p-p38/p38, and pAkt/Akt compared to the LPS group ($p < 0.05$) (Fig. 7(A-D)). These results suggest that the three phenylbutenoids and PE markedly suppress the activation of the inflammatory response through modulation of ERK, p38 MAPK, and Akt pathways.

Preventive effect on damaged C2C12 myoblast cells

Effect of three phenylbutenoids and PE on H_2O_2-induced ROS generation in C2C12 myoblast cells

The levels of ROS were determined in C2C12 myoblast cells after pretreatment with three phenylbutenoids and PE for 24 h, followed by exposure to H_2O_2 for 2 h. Intracellular ROS production in the H_2O_2-treated group significantly increased to 159.2–165.5% compared to the normal control group. However, the three phenylbutenoids and PE significantly suppressed the production of ROS (Fig. 8(A-D); $p < 0.05$). These results indicate that the three phenylbutenoids and PE can significantly reduce cell damage by inhibiting the generation of ROS.

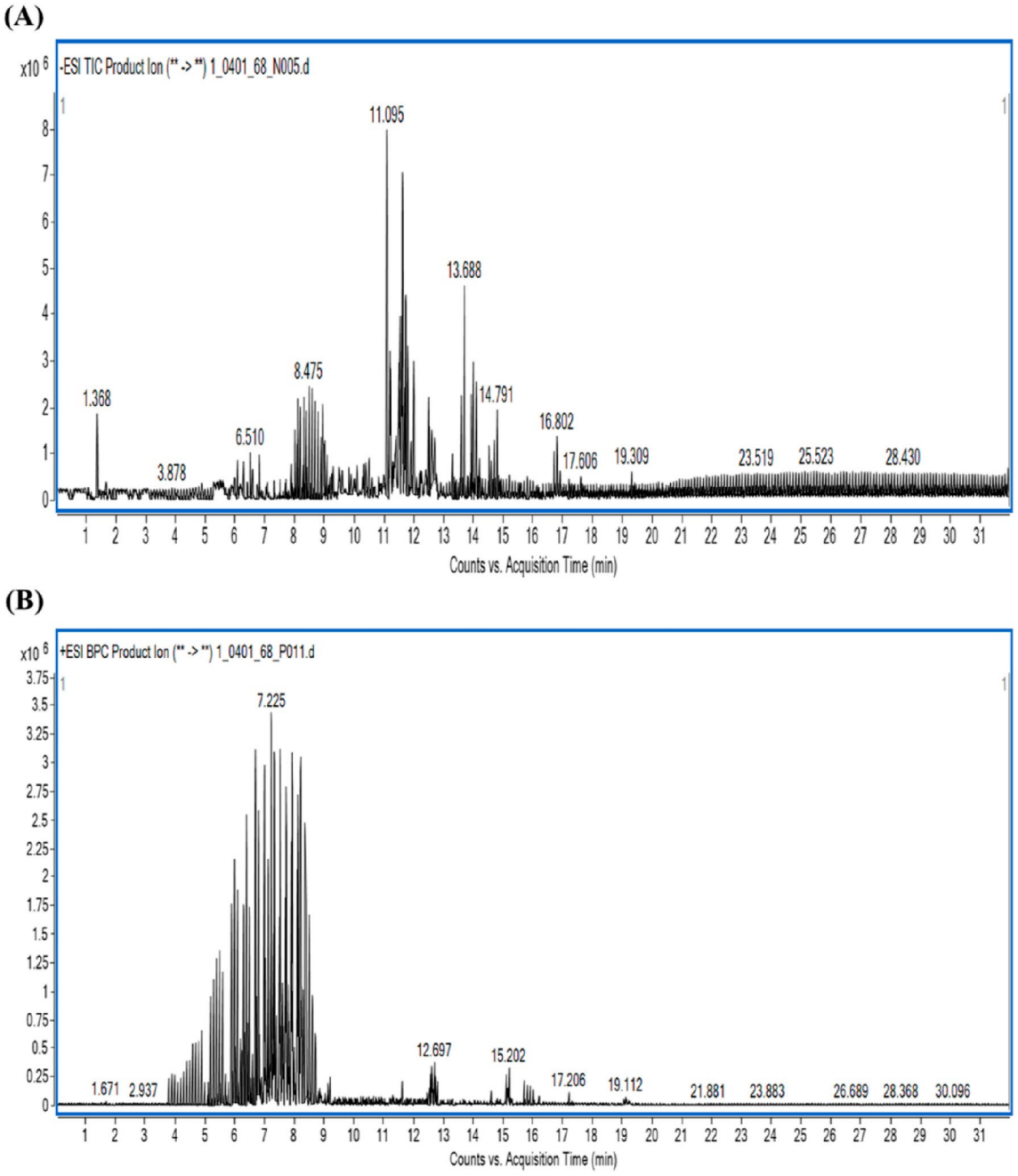

Fig. 2 LC-MS-MS chromatograms of PE. (**A**) negative mode, (**B**) positive mode

Three phenylbutenoids and PE inhibit apoptosis in H_2O_2-induced C2C12 myoblast cells through the caspase-3 pathway

Exposure to H_2O_2 markedly elevated the proportion of apoptotic cells in C2C12 myoblast cells. However, pre-treatment with the three phenylbutenoids and PE provided a protective effect against H_2O_2-induced apoptosis (Fig. 9(A-D)). According to the Hoechst 33342 staining assay, all test samples significantly reduced the percentage of apoptotic cells in C2C12 myoblasts (Additional file 1: Fig. S2 and Fig. 9(A-D)). However, PE and DMPBD demonstrated potent anti-apoptotic effects, with IC_{50} values of 11.6 and 12.4 μg/mL, respectively (Table 4). As shown in Fig. 9(E-F), the ratio of cleaved caspase-3 to pro-caspase-3 was significantly upregulated after treatment with H_2O_2. All compounds and PE treatment significantly reduced the relative cleaved-caspase-3 to pro-caspase-3 ratio ($p < 0.05$). In contrast, there were no notable differences in the expression levels of Bax/Bcl-2 between the experimental groups (Fig. 9(E-F); $p < 0.05$).

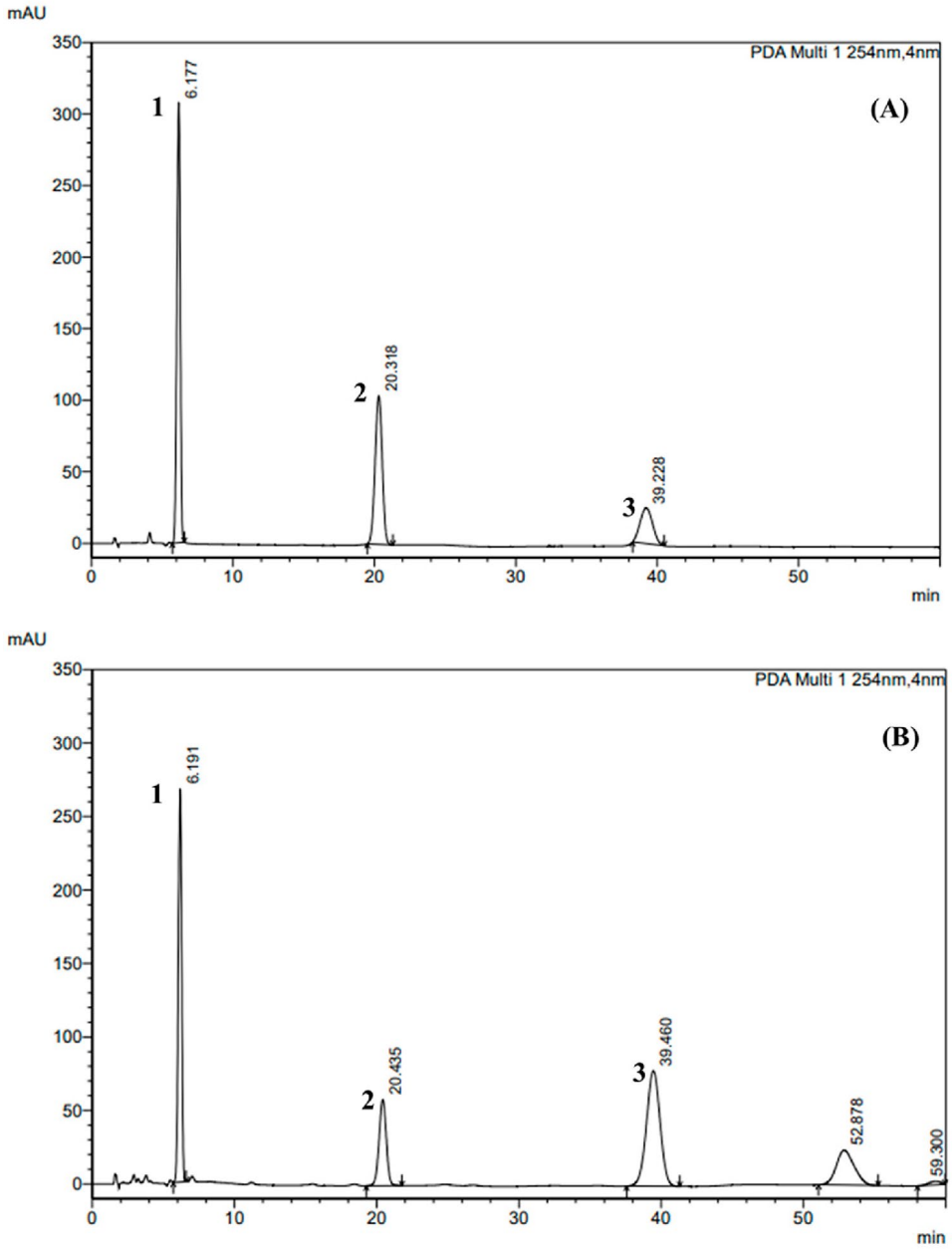

Fig. 3 HPLC chromatograms of authentic phenylbutenoids (**A**) and PE (**B**); 1: (*E*)-1-(3,4-dimethoxyphenyl)but-3-en-1-ol (compound D), 2: (*E*)-1-(3,4-dimethoxyphenyl)but-3-en-1-yl acetate (compound D acetate), and 3: (*E*)-(3,4-dimethoxyphenyl)butadiene (DMPBD)

Table 2 Concentration of phenylbutenoids in PE

Phenylbutenoids	Concentration (% w/w)
Compound D	0.28 ± 0.004
Compound D acetate	0.21 ± 0.003
DMPBD	0.93 ± 0.024

The results are expressed as mean ± SD ($n = 4$). Compound D: (*E*)-1-(3,4-dimethoxyphenyl)but-3-en-1-ol; Compound D acetate: (*E*)-1-(3,4-dimethoxyphenyl)but-3-en-1-yl acetate; DMPBD: (*E*)-(3,4-dimethoxyphenyl) butadiene

These findings indicate that the three phenylbutenoids and PE may effectively suppress the activation of the apoptosis response via the caspase-3 pathway.

Discussion

Muscle injuries, which may result from contusion, strain, or laceration, often lead to inflammation and pain. The infiltration of inflammatory cells triggers the inflammatory response. This response can occur in any tissue after trauma, infection, post-ischemic events, toxic exposure, or autoimmune injuries [24]. Therapeutic

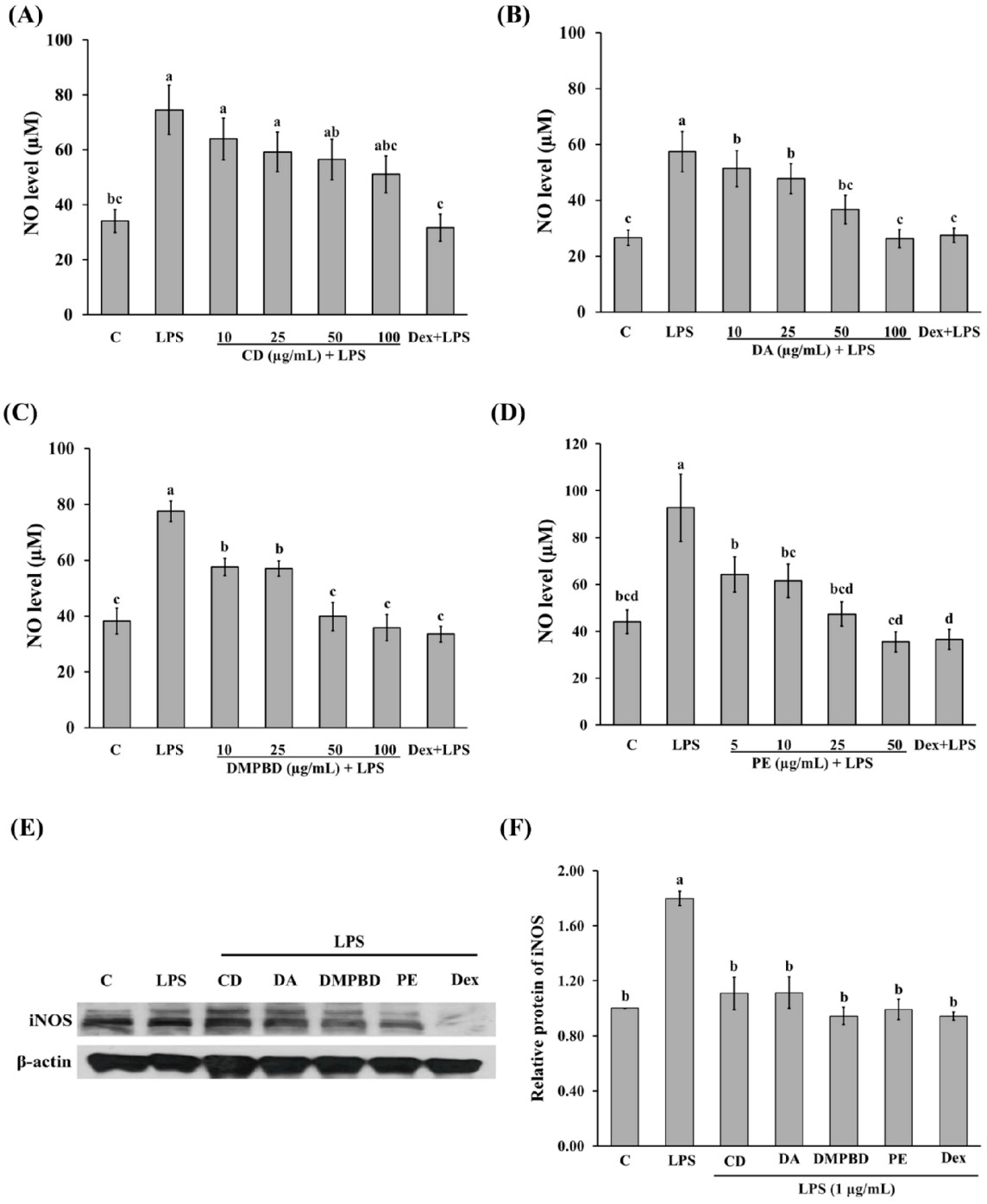

Fig. 4 Inhibitory effects of three phenylbutenoids and PE on NO production and iNOS expression in LPS-induced inflammation in RAW264.7 macrophages. Secretion levels of NO following treatment with (**A**) compound D, (**B**) compound D acetate, (**C**) DMPBD, (**D**) PE, (**E**) western blot analysis showing iNOS protein bands in response to compound D, compound D acetate, DMPBD, and PE treatments, and (**F**) Relative expression of iNOS protein. All values are presented as the mean ± SEM from four independent experiments ($n = 4$). Different lowercase letters indicate significant differences between samples at $p < 0.05$, as determined by ANOVA followed by LSD post-hoc test. CD: (*E*)-1-(3,4-dimethoxyphenyl)but-3-en-1-ol (compound D), DA: (*E*)-1-(3,4-dimethoxyphenyl)but-3-en-1-yl acetate (compound D acetate), DMPBD: (*E*)-(3,4-dimethoxyphenyl)butadiene, PE: phenylbutenoid extract, Dex: dexamethasone, LPS: lipopolysaccharide

Table 3 Inhibitory effects of PE and three phenylbutenoids on NO, TNF-α, and IL-1β production in LPS-induced RAW264.7 cells

Compound/Extract	IC_{50} (μg/mL)		
	Inhibition of NO	Inhibition of TNF-α	Inhibition of IL-1β
Compound D	51.8 ± 4.3^{d}	52.8 ± 4.5^{c}	47.6 ± 3.5^{c}
Compound D acetate	36.2 ± 2.8^{c}	39.6 ± 1.6^{b}	32.2 ± 2.6^{b}
DMPBD	16.3 ± 0.6^{b}	37.2 ± 1.2^{b}	17.7 ± 1.2^{a}
PE	7.2 ± 0.4^{a}	23.4 ± 1.9^{a}	19.8 ± 1.6^{a}

The results are expressed as mean ± SEM ($n = 4$). Statistical analysis was performed using one-way ANOVA followed by LSD post-hoc test. Significant differences within each column are indicated by different letters ($p < 0.05$). Dexamethasone (1 μg/mL) showed 99.4 ± 3.8% inhibition of NO, 87.3 ± 8.7% inhibition of TNF-α, and 96.2 ± 1.9% inhibition of IL-1β. NO: nitric oxide, TNF-α: tumor necrosis factor-α, IL-1β: interleukin-1β, compound D: (*E*)-1-(3,4-dimethoxyphenyl)but-3-en-1-ol, compound D acetate: (*E*)-1-(3,4-dimethoxyphenyl)but-3-en-1-yl acetate, DMPBD: (*E*)-(3,4-dimethoxyphenyl)butadiene, PE: phenylbutenoid extract

interventions typically consist of both non-pharmacological and pharmacological approaches. Nevertheless, some conventional treatments may result in adverse effects [25]. Therefore, it is essential to explore effective herbal remedies for managing inflammation and muscle injuries. In the present study, PE from the rhizomes of *Z. cassumunar* was prepared using a green microwave extraction method with PEG 400. This method was found to be beneficial for both health and environment due to minimize the use of harmful solvents and reduce energy consumption [26]. By employing this environmentally friendly extraction technique, we can enhance the sustainability of the extraction process while preserving the bioactive compounds in the plant material. In the present study, the obtained extract contained a total phenylbutenoid content of 1.42% w/w, which included 0.93% w/w of DMPBD, 0.28% w/w of compound D, and 0.21% w/w of compound D acetate. The main three contents found in our study were consistent with those previously reported by Kaewchoothong et al. [18]. Unfortunately, a dimeric phenylbutenoid, namely

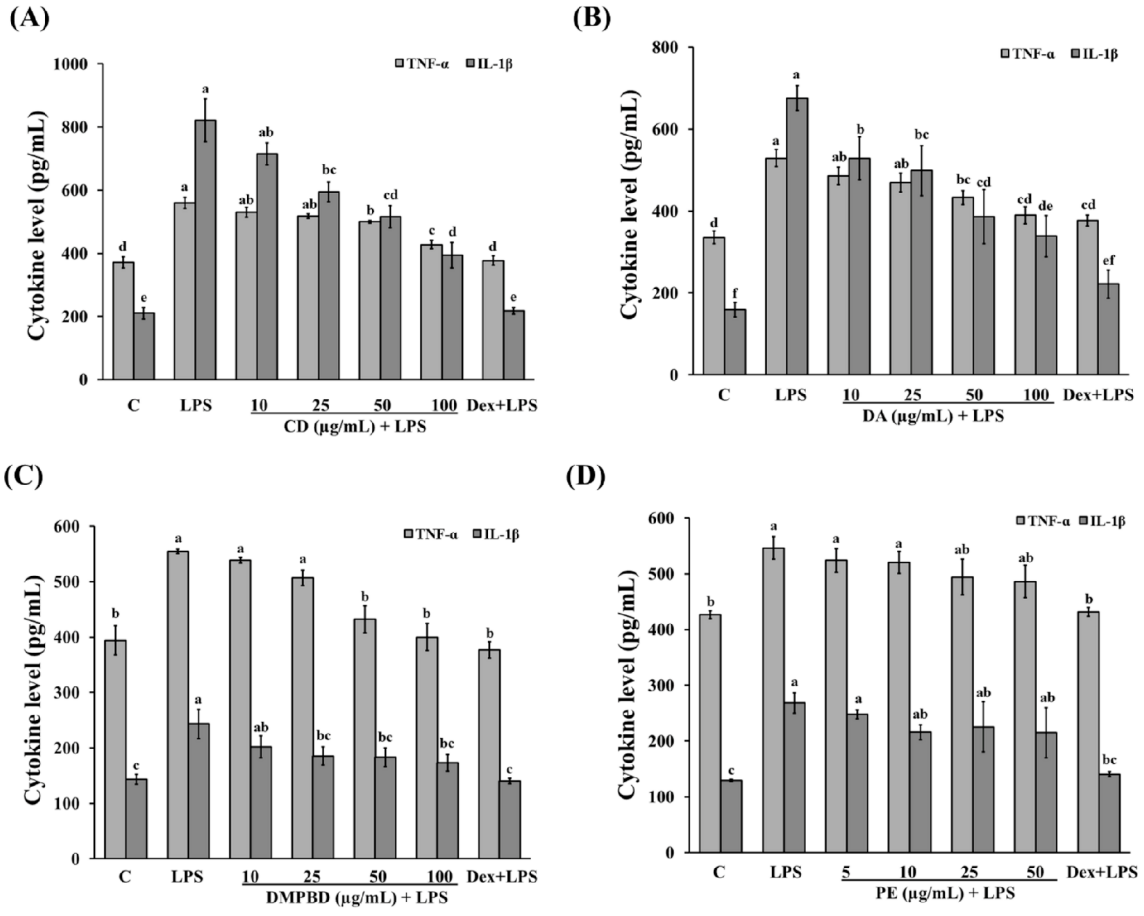

Fig. 5 Inhibition of TNF-α and IL-1β secretion by compound D, compound D acetate, DMPBD, and PE in LPS-induced inflammation in RAW264.7 macrophages. Secretion levels of TNF-α and IL-1β following treatment with (**A**) compound D, (**B**) compound D acetate, (**C**) DMPBD, and (**D**) PE. All values are presented as the mean ± SEM from four independent experiments ($n = 4$). Different lowercase letters indicate significant differences between samples at $p < 0.05$, as determined by ANOVA followed by LSD post-hoc test. CD: (*E*)-1-(3,4-dimethoxyphenyl)but-3-en-1-ol (compound D), DA: (*E*)-1-(3,4-dimethoxyphenyl)but-3-en-1-yl acetate (compound D acetate), DMPBD: (*E*)-(3,4-dimethoxyphenyl)butadiene, PE: phenylbutenoid extract, Dex: dexamethasone, LPS: lipopolysaccharide

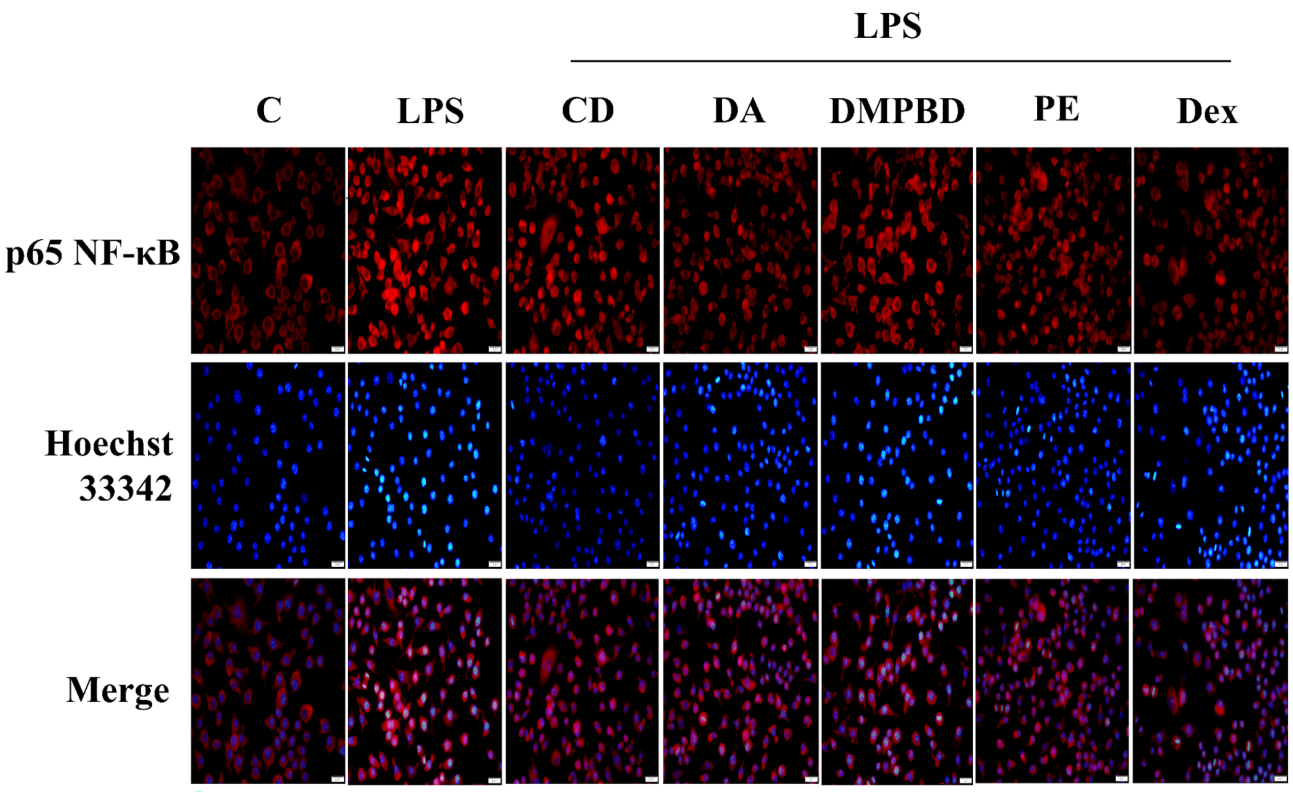

Fig. 6 Effect of compound D, compound D acetate, DMPBD, and PE on p65 NF-κB translocation in LPS-inflamed RAW264.7 macrophages. Immunofluorescence staining for NF-κB p65 was observed under fluorescence microscopy after treatment with all tested compounds in the presence and absence of LPS. Nuclei were visualized using Hoechst 33342. CD: (*E*)-1-(3,4-dimethoxyphenyl)but-3-en-1-ol (compound D), DA: (*E*)-1-(3,4-dimethoxyphenyl)but-3-en-1-yl acetate (compound D acetate), DMPBD: (*E*)-(3,4-dimethoxyphenyl)butadiene, PE: phenylbutenoid extract, Dex: dexamethasone, LPS: lipopolysaccharide

(*E*)-3-(3,4-dimethoxyphenyl)-4-[(*E*)-3,4-dimethoxystyryl] cyclohex-1-ene, which is a naturally potent NO inhibitor found in *Z. cassumunar*, was not detected in PE. This may be attributed to its higher lipophilicity than PEG 400 and its lower concentration in *Z. cassumunar*. This dimeric compound could be extracted by using hexane and detected after solvent evaporation, as suggested by Kaewchoothong et al. [18]. Microwave extraction serves as a superior alternative to conventional extraction methods, as it requires less time, uses fewer solvents, achieves a higher extraction rate, and yields better products with minimal loss. Additionally, it reduces the risk of decomposition and oxidation of phytoconstituents [27]. Moreover, the ultra-high-performance liquid chromatography-triple/time-of-flight mass spectrometry (UHPLC-QTOF-MS/MS) analysis of the PE revealed the presence of several compounds, including DMPBD, which has been identified as a major anti-inflammatory constituent. The signals from peak numbers 2 and 3 both exhibit positive quasi-molecular $[M^+H]^+$ ions at m/z 191 (molecular weight 190 Da), corresponding to a molecular formula of $C_{12}H_{14}O_2$ [28].

Macrophages play a crucial role in skeletal muscle injury and repair, acting as key regulators of inflammation and facilitating the regeneration process [29]. PE was evaluated for its anti-inflammatory activities by determining its inhibitory effects on the levels of TNF-α, IL-1β, and NO in RAW264.7 cells, in comparison to three active marker compounds. LPS was used to stimulate RAW264.7 cells, thereby triggering the generation of pro-inflammatory mediators [10]. The results indicated that PE exhibited the most potent inhibition of NO production compared to DMPBD, compound D, and compound D acetate, with an IC_{50} value of 7.2 μg/mL. Additionally, PE was linked to the downregulation of iNOS enzyme expression, despite having a low concentration of total phenylbutenoids (1.42% w/w). Although PE did not contain the aforementioned potent dimeric NO inhibitor, our findings are consistent with previous study demonstrating the inhibitory effects of phenylbutenoid-enriched *Z. cassumunar* extracts (PZEs) against NO production. These findings suggest that PZEs were more effective than their four marker compounds [18]. Furthermore, our study found that PE exhibited the highest inhibition of TNF-α secretion. PE and DMPBD demonstrated comparable suppression of IL-1β secretion, with IC_{50} values of 19.8 and 17.7 μg/mL, respectively. Their activities were also greater than those of compound

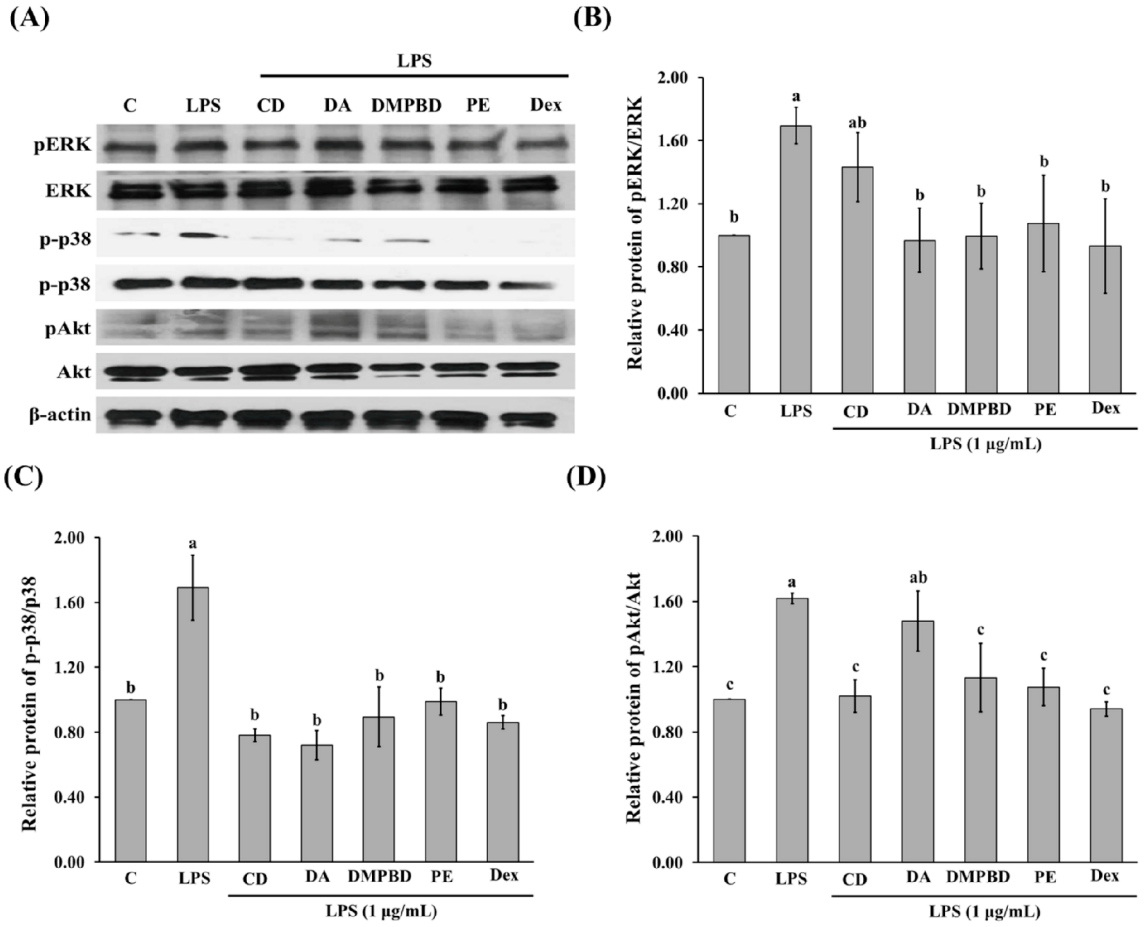

Fig. 7 Suppression of Akt, ERK, and p38MAPK signaling pathways by compound D, compound D acetate, DMPBD, and PE in LPS-induced inflammation in RAW264.7 macrophages. (**A**) Western blot analysis of ERK, p38 MAPK, and Akt protein bands in response to all phenylbutenoids and PE treatment, (**B**) Relative expression of p-ERK/ERK protein, (**C**) Relative expression of p-p38/p38 protein, and (**D**) Relative expression of p-Akt/Akt protein. All values are presented as the mean ± SEM from four independent experiments ($n = 4$). Different lowercase letters indicate significant differences between samples at $p < 0.05$, as determined by ANOVA followed by LSD post-hoc test. CD: (*E*)-1-(3,4-dimethoxyphenyl)but-3-en-1-ol (compound D), DA: (*E*)-1-(3,4-dimethoxyphenyl)but-3-en-1-yl acetate (compound D acetate), DMPBD: (*E*)-(3,4-dimethoxyphenyl)butadiene, PE: phenylbutenoid extract, Dex: dexamethasone, LPS: lipopolysaccharide

D and compound D acetate. However, no previous studies have reported the effects of PE, DMPBD, and compound D acetate on the secretion of TNF-α and IL-1β. Among these compounds, only compound D has shown anti-inflammatory activity involving a reduction in both gene and protein expression of IL-1β in a primary cell culture of synovial fibroblasts [30]. Therefore, our study indicates that PE and the three main compounds found in PE exhibit anti-inflammatory activity by inhibiting the release of pro-inflammatory mediators; however, PE has the highest potency against inflammation. The inhibitory effects of PE against pro-inflammatory mediators, including NO, TNF-α, and IL-1β, might result from the three main compounds (DMPBD, compound D, and compound D acetate) found in PE.

The NF-κB transcription factor family is pivotal in mediating inflammatory responses; thus, targeting the inhibition of NF-κB activation is a key therapeutic strategy for reducing severe inflammatory reactions [7]. In addition to the NF-κB pathway, the p38, ERK, and Akt pathways have also been identified as crucial in the expression of numerous pro-inflammatory genes [8]. The results of this study indicate that all tested compounds inhibit the translocation of NF-κB p65 into the nucleus. Furthermore, our findings suggest that PE and the three phenylbutenoids partially inhibit the phosphorylation of ERK1/2 and p38 MAPK. However, PE, DMPBD, and compound D demonstrated inhibitory effects on the activation of Akt, whereas compound D acetate did not inhibit this signaling protein. Taken together, the anti-inflammatory activity of PE could be due to the suppression of NF-κB, MAPK (ERK1/2 and p38), and Akt pathways, leading to the suppression of the inflammatory response. Our research is the first to demonstrate that PE and its key compounds suppress inflammation by regulating the NF-κB, MAPK (ERK1/2 and p38), and Akt

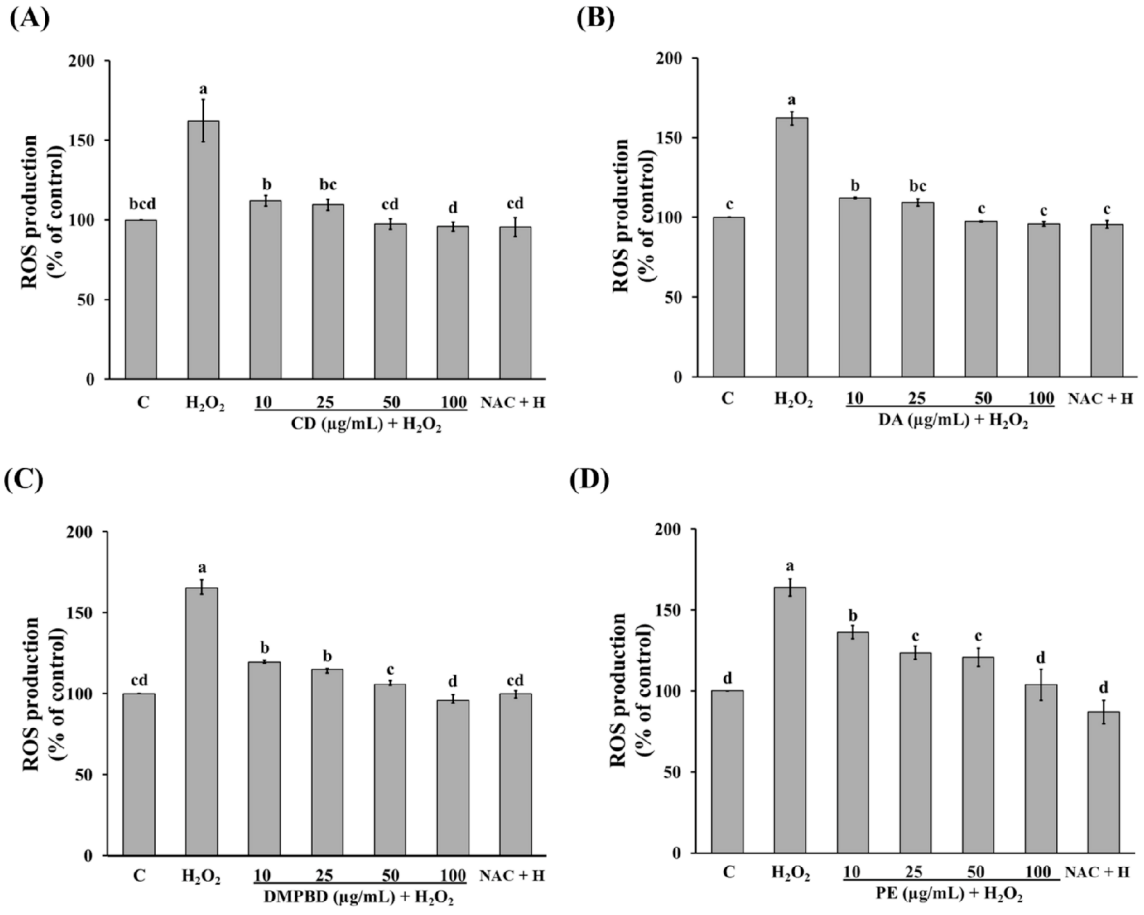

Fig. 8 Inhibition of ROS production in C2C12 myoblast cells treated with H_2O_2 and various compounds, as measured by the $DCFH_2$-DA assay. Panels show ROS production following treatment with (**A**) compound D, (**B**) compound D acetate, (**C**) DMPBD, and (**D**) PE. All data are expressed as the mean ± SEM from four independent experiments ($n = 4$). Different lowercase letters indicate significant differences between samples at $p < 0.05$, as determined by ANOVA followed by LSD post-hoc test. CD: (*E*)-1-(3,4-dimethoxyphenyl)but-3-en-1-ol (compound D), DA: (*E*)-1-(3,4-dimethoxyphenyl)but-3-en-1-yl acetate (compound D acetate), DMPBD: (*E*)-(3,4-dimethoxyphenyl)butadiene, PE: phenylbutenoid extract, NAC: N-acetylcysteine

signaling pathways. NF-κB serves as a central mediator of inflammation, while MAPK pathways amplify the inflammatory signals, and Akt provides a critical link between growth factor signaling and inflammatory responses [8, 31].

ROS play a crucial role in muscle injury and repair. Elevated ROS levels can cause oxidative stress, damage cellular components, and impair muscle function, which contribute to muscle atrophy [32, 33]. The increased levels of ROS can lead to oxidative stress, thereby triggering early events in the apoptotic pathway in skeletal muscle cells [34]. This study is the first to demonstrate the important role of PE and its marker compounds in regulating muscle injury. Pre-treatment with three phenylbutenoids and PE suppressed the activation of the apoptotic pathway in C2C12 cells triggered by H_2O_2. Notably, PE and DMPBD exhibited the most potent and comparable inhibitory effects on apoptosis, with IC_{50} values of 11.6 and 12.4 μg/mL, respectively, as well as on ROS production in C2C12 myoblast cells. A reduction in apoptosis was associated with the suppression of H_2O_2-stimulated ROS production in C2C12 myoblasts, suggesting that the protective effects of PE and its marker compounds are associated with the alleviation of oxidative stress [35]. Phenylbutenoids are phenolic substances characterized by the presence of an aromatic ring that is bonded to one or more hydroxyl groups. Phenolic compounds are antioxidants specified by their ability to capture free radicals and ROS [36]. PE exhibited higher ROS inhibitory activity than its marker compounds, probably due to its diverse chemical composition and synergistic effects [37]. Caspase-3 is a key mediator of apoptosis in muscle injury, contributing to cell death and atrophy. Inhibiting its activity may enhance muscle regeneration and function after injury [12, 38]. All tested compounds and PE treatment significantly reduced the ratio of cleaved-caspase-3 to pro-caspase-3. Moreover, these results suggest that the three phenylbutenoids and PE have the potential to significantly inhibit apoptosis by modulating the caspase-3 pathway. This finding indicates that these compounds can

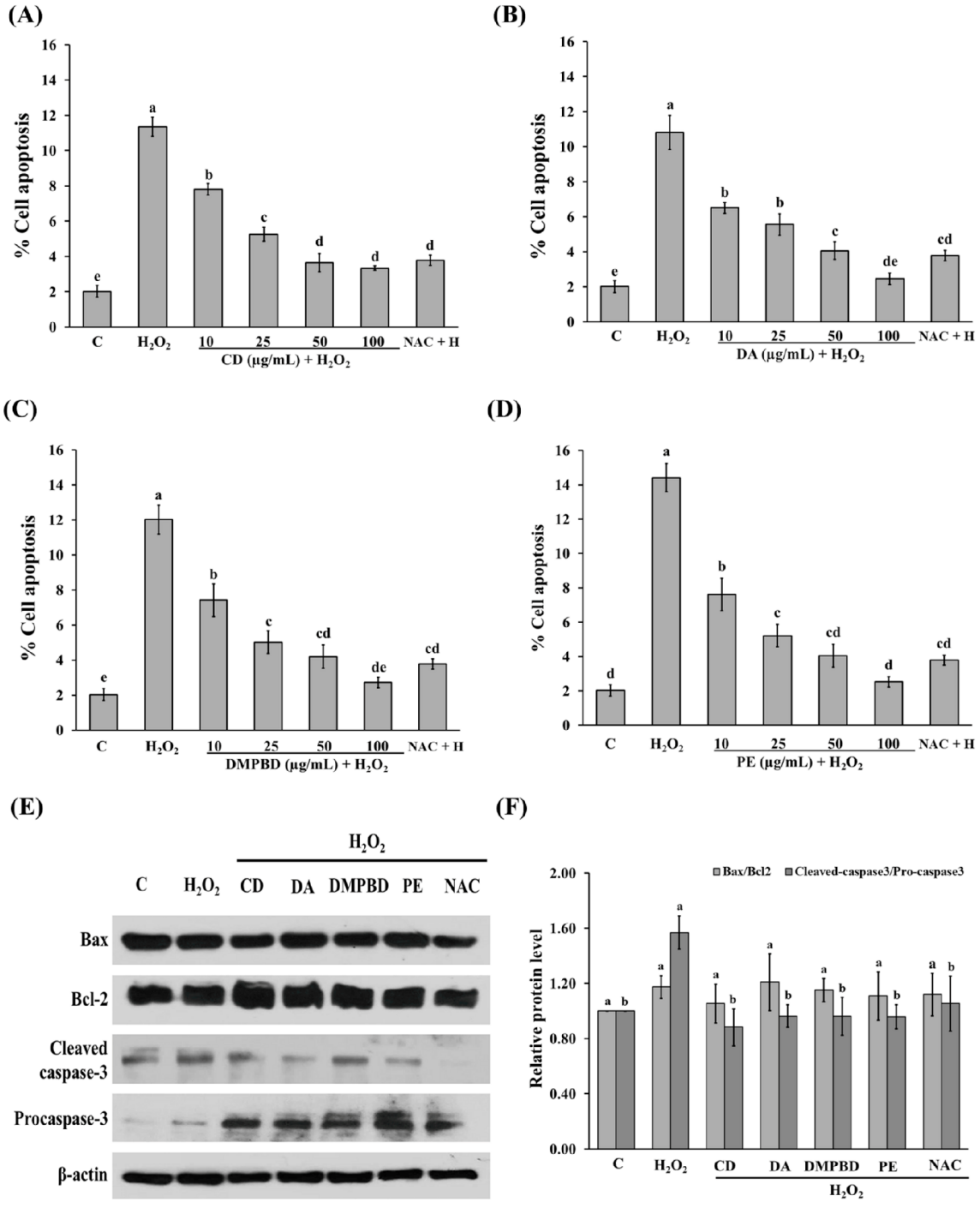

Fig. 9 Effects of compound D, compound D acetate, DMPBD, and PE on H_2O_2 -induced apoptosis in C2C12 myoblast cells. Panels show the percentage of cell apoptosis following treatment with (**A**) compound D, (**B**) compound D acetate, (**C**) DMPBD, (**D**) PE, (**E**) western blot analysis of Bax, Bcl2, cleaved caspase-3, and procaspase-3 protein bands in response to all phenylbutenoids and PE, and (**F**) Relative expression of Bax/Bcl2 and cleaved caspase-3/procaspase-3 protein levels. All data are presented as the mean ± SEM from four independent experiments ($n = 4$). Different lowercase letters indicate significant differences between samples at $p < 0.05$, as determined by ANOVA followed by LSD post-hoc test. CD: (*E*)-1-(3,4-dimethoxyphenyl)but-3-en-1-ol (compound D), DA: (*E*)-1-(3,4-dimethoxyphenyl)but-3-en-1-yl acetate (compound D acetate), DMPBD: (*E*)-(3,4-dimethoxyphenyl)butadiene, PE: phenylbutenoid extract, NAC: N-acetylcysteine

Table 4 Protective effects of PE and three phenylbutenoids against H_2O_2-induced apoptosis in C2C12 myoblast cells

Compound/Extract	IC_{50} (μg/mL)
	Inhibition of apoptosis
Compound D	23.7 ± 2.5[b]
Compound D acetate	20.7 ± 1.0[b]
DMPBD	12.4 ± 0.7[a]
PE	11.6 ± 0.6[a]

The results are expressed as mean ± SEM ($n = 4$). Statistical analysis was performed using one-way ANOVA followed by LSD post-hoc test. Significant differences among all samples are indicated by different letters in each column ($p < 0.05$). NAC (50 mM) exhibited 77.29 ± 0.97% inhibition of apoptosis. Compound D: (*E*)-1-(3,4-dimethoxyphenyl)but-3-en-1-ol, compound D acetate: (*E*)-1-(3,4-dimethoxyphenyl)but-3-en-1-yl acetate, DMPBD: (*E*)-(3,4-dimethoxyphenyl)butadiene, PE: phenylbutenoid extract

effectively interfere with key apoptotic signaling mechanisms, potentially offering protective effects against cell death induced by oxidative stress [23, 39].

Conclusion

The present study revealed that PE, which contains 1.42% w/w total phenylbutenoids and was extracted using green microwave extraction, demonstrates significant anti-inflammatory and anti-apoptotic properties. PE reduced NO levels by inhibiting iNOS protein expression and decreased the levels of the cytokines IL-1β and TNF-α. It also alleviated inflammation in LPS-stimulated macrophages by blocking the activation of the Akt, ERK, and p38 MAPK signaling pathways. Additionally, PE effectively inhibited H_2O_2-induced ROS generation and prevented apoptotic cell death in muscle cells. Furthermore, the three phenylbutenoids and PE significantly inhibited apoptosis by affecting the caspase-3 pathway. These results indicate that PE could be a promising alternative treatment for muscle injuries related to musculoskeletal disorders. Nonetheless, additional in vivo studies are needed to evaluate its effectiveness, safety, and optimal dosage.

Supplementary Information

The online version contains supplementary material available at https://doi.org/10.1186/s12906-025-04907-w.

Supplementary Material 1

Acknowledgements
The authors wish to thank Dr. Fredrick Eze for assistance with English editing.

Author contributions
P.P. and W.S. conceived and designed the research study and T.G. performed the experiments and wrote the first draft of the manuscript. PP, WS and TG analyzed the data, discussed the findings, and prepared the manuscript. All authors revised and approved the submitted version of manuscript.

Funding
This research was financially supported by the Thailand Research Fund through the Royal Golden Jubilee Ph.D. Program (grant number PHD/0038/2558).

Data availability
Data is provided within the manuscript or supplementary information files.

Declarations

Ethics approval and consent to participate
There are no studies in our article that require ethics committee approval.

Consent for publication
Not applicable.

Patents
This work received petty patent application number 2003002885 for the topic "Preparation of Phenylbutenoid Extract from *Zingiber cassumunar* Rhizome Using a Green Extraction Method."

Competing interests
The authors declare no competing interests.

Author details
[1]Department of Pharmacognosy and Pharmaceutical Botany, Faculty of Pharmaceutical Sciences, Prince of Songkla University, Hat-Yai 90112, Songkhla, Thailand
[2]Division of Health and Applied Sciences, Faculty of Science, Prince of Songkla University, Hat-Yai, Songkhla 90112, Thailand
[3]Phytomedicine and Pharmaceutical Biotechnology Research Center, Faculty of Pharmaceutical Sciences, Prince of Songkla University, Hat-Yai, Songkhla 90112, Thailand

Received: 16 December 2024 / Accepted: 29 April 2025
Published online: 16 May 2025

References

1. Cieza A, Causey K, Kamenov K, Hanson SW, Chatterji S, Vos T. Global estimates of the need for rehabilitation based on the global burden of disease study 2019: a systematic analysis for the global burden of disease study 2019. Lancet. 2020;396(10267):2006–17.
2. GBD 2021 Other Musculoskeletal Disorders Collaborators. Global, regional, and National burden of other musculoskeletal disorders, 1990–2020, and projections to 2050: a systematic analysis of the global burden of disease study 2021. Lancet Rheumatol. 2023;5(11):e670–82.
3. Duan H, Chen S, Mai X, Fu L, Huang L, Xiao L, et al. Low-intensity pulsed ultrasound (LIPUS) promotes skeletal muscle regeneration by regulating PGC-1α/AMPK/GLUT4 pathways in satellite cells/myoblasts. Cell Signal. 2024;117:111097.
4. Choi YH. Schisandrin A prevents oxidative stress-induced DNA damage and apoptosis by attenuating ROS generation in C2C12 cells. Biomed Pharmacother. 2018;106:902–9.
5. Gupta P, Dutt V, Kaur N, Kalra P, Gupta S, Dua A, et al. S-allyl cysteine: A potential compound against skeletal muscle atrophy. Biochim Biophys Acta Gen Subj. 2020;1864(10):129676.
6. Nie Y, Cai S, Yuan R, Ding S, Zhang X, Chen L, et al. Zfp422 promotes skeletal muscle differentiation by regulating EphA7 to induce appropriate myoblast apoptosis. Cell Death Differ. 2020;27(5):1644–59.
7. Yi X, Tao J, Qian Y, Feng F, Hu X, Xu T, et al. Morroniside ameliorates inflammatory skeletal muscle atrophy *via* inhibiting canonical and non-canonical NF-κB and regulating protein synthesis/degradation. Front Pharmacol. 2022;13:1056460.
8. Xiao K, Liu C, Tu Z, Xu Q, Chen S, Zhang Y, et al. Activation of the NF-κB and MAPK signaling pathways contributes to the inflammatory responses, but not cell injury, in IPEC-1 cells challenged with hydrogen peroxide. Oxid Med Cell Longev. 2020;2020:5803639.
9. Fang Y, Yang L, He J. Plantanone C attenuates LPS-stimulated inflammation by inhibiting NF-κB/iNOS/COX-2/MAPKs/Akt pathways in RAW 264.7 macrophages. Biomed Pharmacother. 2021;143:112104.
10. Sukketsiri W, Tanasawet S, Moolsap F, Tantisira MH, Hutamekalin P, Tipmanee V, et al. ECa 233 suppresses LPS-induced Proinflammatory responses in macrophages via suppressing ERK1/2, p38 MAPK, and Akt pathways. Biol Pharm Bull. 2019;42(8):1358–65.

11. Guan K, Qi X, Chen H, Ma Y. The cytoprotection of milk-derived MFG-E8 on mitochondria-injured L6 cell via mediation of Akt/bcl-2/bax-caspase-3 signaling pathway. Food Biosci. 2023;51:102289.
12. Zhang M, Wang X, Bai B, Zhang R, Li Y, Wang Y. Oxymatrine protects against sepsis-induced myocardial injury via Inhibition of the TNF-α/p38-MAPK/caspase-3 signaling pathway. Mol Med Rep. 2016;14(1):551–9.
13. Jeenapongsa R, Yoovathaworn K, Sriwatanakul KM, Pongprayoon U, Sriwatanakul K. Anti-inflammatory activity of (*E*)-1-(3, 4-dimethoxyphenyl) butadiene from *Zingiber cassumunar* Roxb. J Ethnopharmacol. 2003;87(2–3):143–8.
14. Masuda T, Jitoe A, Mabry TJ. Isolation and structure determination of cassumunarins A, B, and C: New anti-inflammatory antioxidants from a tropical ginger, *Zingiber cassumunar*. J Am Oil Chem Soc. 1995;72:1053-7.
15. Ozaki Y, Kawahara N, Harada M. Anti-inflammatory effect of *Zingiber cassumunar* Roxb. And its active principles. Chem Pharm Bull. 1991;39(9):2353–6.
16. Panthong A, Kanjanapothi D, Niwatananant W, Tuntiwachwuttikul P, Reutrakul V. Anti-inflammatory activity of compound D {(*E*)-4-(3′, 4′-dimethoxyphenyl) but-3-en-2-ol} isolated from *Zingiber cassumunar* Roxb. Phytomedicine. 1997;4(3):207–12.
17. Han AR, Kim MS, Jeong YH, Lee SK, Seo EK. Cyclooxygenase-2 inhibitory phenylbutenoids from the rhizomes of *Zingiber cassumunar*. Chem Pharm Bull. 2005;53(11):1466–8.
18. Kaewchoothong A, Tewtrakul S, Panichayupakaranant P. Inhibitory effect of phenylbutanoid-rich *Zingiber cassumunar* extracts on nitric oxide production by murine macrophage-like RAW264.7 cells. Phytother Res. 2012;26(12):1789–92.
19. Pongprayoon U, Soontornsaratune P, Jarikasem S, Sematong T, Wasuwat S, Claeson P. Topical antiinflammatory activity of the major lipophilic constituents of the rhizome of *Zingiber cassumunar*. Part I: the essential oil. Phytomedicine. 1997;3(4):319–22.
20. Leelarungrayub D, Suttajit M. Potential antioxidant and anti-inflammatory activities of Thai Plai (*Zingiber cassumunar* Roxb.) essential oil. Int J Essen Oil Ther. 2009;3:25–30.
21. Azadbakht M, Nayebi E, Fard RE, Fatemeh K. Standardization and formulation of an herbal appetite-stimulating drug from *Gentiana Olivieri*. J Herb Med. 2020;19:100306.
22. Crinnion WJ. The CDC fourth National report on human exposure to environmental chemicals: what it tells Us about our toxic burden and how it assists environmental medicine physicians. Altern Med Rev. 2010;15(2):101–9.
23. Sukketsiri W, Sawangjaroen K, Tanasawet S. Anti-apoptotic effects of phyllanthin against alcohol-induced liver cell death. Trop J Pharm Res. 2016;15(5):981–8.
24. Xie DG, Li JH, Zhong YL, Han H, Zhang JJ, Zhang ZQ, et al. Role of TRPC6 in apoptosis of skeletal muscle ischemia/reperfusion injury. Cell Signal. 2024;121:111289.
25. de Sire A, Marotta N, Lippi L, Scaturro D, Fari G, Liccardi A, et al. Pharmacological treatment for acute traumatic musculoskeletal pain in athletes. Medicina. 2021;57(11):1208.
26. Kumar M, Barbhai MD, Puranik S, Radha, Natta S, Senapathy M, et al. Combination of green extraction techniques and smart solvents for bioactives recovery. TrAC Trends Anal Chem. 2023;169:117286.
27. Koparde AA, Magdum CS. Conventional and microwave assisted extraction of *Eulophia ochreta Lindl* and *Zingiber cassumunar* Roxb: an comparitive account. Res J Pharm Technol. 2014;7(7):746–8.
28. Kabkrathok P, Jarussophon S, Unger O, Lomarat P, Reutrakul V, Pittayanurak P, et al. Mass spectral analysis of secondary metabolites from *Zingiber montanum* rhizome extract using UHPLC-HR-ESI-QTOF-MS/MS. Phytochem Anal. 2022;33(1):57–71.
29. Wang X, Zhao W, Ransohoff RM, Zhou L. Infiltrating macrophages are broadly activated at the early stage to support acute skeletal muscle injury repair. J Neuroimmunol. 2018;317:55–66.
30. Chaiwongsa R, Ongchai S, Boonsing P, Kongtawelert P, Panthong A, Reutrakul V. Active compound of *Zingiber cassumunar* Roxb. down-regulates the expression of genes involved in joint erosion in a human synovial fibroblast cell line. Afr J Tradi Complement Altern Med. 2012;10(1):40–8.
31. Yan Z, Wang Y, Song Y, Ma Y, An Y, Wen R, et al. Phenethylferulate as a natural inhibitor of inflammation in LPS-stimulated RAW 264.7 macrophages: focus on NF-κB, Akt, and MAPK signaling pathways. BMC Complement Med Ther. 2023;23(1):398.
32. Qiu J, Fang Q, Xu T, Wu C, Xu L, Wang L, et al. Mechanistic role of reactive oxygen species and therapeutic potential of antioxidants in denervation-or fasting-induced skeletal muscle atrophy. Front Physiol. 2018;9:215.
33. Agrawal S, Chakole S, Shetty N, Prasad R, Lohakare T, Wanjari M. Exploring the role of oxidative stress in skeletal muscle atrophy: mechanisms and implications. Cureus. 2023;15(7):e42178.
34. Sciorati C, Rigamonti E, Manfredi AA, Revere-Querini P. Cell death, clearance, and immunity in the skeletal muscle. Cell Death Differ. 2016;23(6):927–37.
35. Chen S, Tang Y, Qian Y, Chen R, Zhang L, Wo L, et al. Allicin prevents H_2O_2-induced apoptosis of HUVECs by inhibiting an oxidative stress pathway. BMC Complement Altern Med. 2014;14:1–8.
36. Abraham AB, Panneerselvam M, Ebenezer C, Costa LT, Solomon RV. A theoretical study on radical scavenging activity of phenolic derivatives naturally found within *Alternaria alternata* extract. Org Biomol Chem. 2024;22(10):2059–74.
37. Faúndez X, Báez ME, Martínez J, Zúñiga-López MC, Espinoza J, Fuentes E. Evaluation of the generation of reactive oxygen species and antibacterial activity of honey as a function of its phenolic and mineral composition. Food Chem. 2023;426:136561.
38. Aladaileh SH, Al-Swailmi FK, Abukhalil MH, Shalayel MH. Galangin protects against oxidative damage and attenuates inflammation and apoptosis *via* modulation of NF-κB p65 and caspase-3 signaling molecules in a rat model of diabetic nephropathy. J Physiol Pharmacol. 2021;72(1):35–44.
39. Saetan S, Sukketsiri W, Chonpathompikunlert P, Klaypradit W, Hawangjoo M, Ngasakul N, et al. Antiproliferative and apoptotic effect of tuna blood on human lung cancer A549 cells via p38 MAPKs and Akt pathway. J King Saud Univ Sci. 2023;35(5):102667.

Publisher's note